PNL-5433
1-

NUREG/CR-4218
PNL-5433

LOCA Simulation in the National Research Universal Reactor Program

Postirradiation Examination Results for the Third Materials Experiment (MT-3) - Second Campaign

Prepared by J. H. Haberman

Pacific Northwest Laboratory
Operated by
Battelle Memorial Institute

Prepared for
U.S. Nuclear Regulatory Commission

NUREG/CR-4218
PNL-5433
R3

LOCA Simulation in the National Research Universal Reactor Program

Postirradiation Examination Results for the Third Materials Experiment (MT-3) - Second Campaign

Manuscript Completed: April 1985
Date Published: June 1985

Prepared by
J. H. Haberman

Pacific Northwest Laboratory
Richland, WA 99352

Prepared for
Division of Accident Evaluation
Office of Nuclear Regulatory Research
U.S. Nuclear Regulatory Commission
Washington, D.C. 20555
NRC FIN B2277

ACKNOWLEDGMENTS

The author would like to thank Chalk River Nuclear Laboratories (CRNL), especially R. J. Chenier, R. R. Edler, I. A. Lusk, and D. M. Schreiter for their major contribution in performing the extensive postirradiation examination. In addition, the author would like to thank R. R. Lewis for overseeing the post-irradiation examination.

ACKNOWLEDGMENTS

The author would like to thank Chalk River Nuclear Laboratories (CRNL), especially C. W. Chenier, R. F. Eadie, W. A. Luska and D. M. Schnelter for their major contribution in performing the extensive postirradiation examinations. In addition, the author would like to thank R. R. Lewis for overseeing the postirradiation examination.

ABSTRACT

A series of in-reactor experiments were conducted using full-length 32-rod pressurized water reactor (PWR) fuel bundles as part of the Loss-of-Coolant Accident (LOCA) Simulation Program by Pacific Northwest Laboratory (PNL). The third materials test (MT-3) was the sixth experiment in a series of thermal-hydraulic and materials deformation/rupture experiments conducted in the National Research Universal (NRU) Reactor, Chalk River, Ontario, Canada. The MT-3 experiment was jointly funded by the U.S. Nuclear Regulatory Commission (NRC) and the United Kingdom Atomic Energy Authority (UKAEA) with the main objective of evaluating ballooning and rupture during active two-phase cooling at elevated temperatures. All 12 test rods in the center of the 32-rod bundle failed with an average peak strain of 55.4%.

At the request of the UKAEA, a destructive postirradiation examination (PIE) was performed on 7 of the 12 test rods. The results of this examination were presented in a previous report. Subsequently, and at the request of UKAEA, PIE was performed on three additional rods along with further examination of one of the previously examined rods. Information obtained from the PIE included cladding thickness measurements, cladding metallography, and particle size analysis of the fractured fuel pellets. This report describes the additional PIE work performed and presents the results of the examinations.

ABSTRACT

A series of in-reactor experiments were conducted using full-length 32-rod pressurized water reactor (PWR) fuel bundles as part of the Loss-of-Coolant Accident (LOCA) Simulation Program by Pacific Northwest Laboratory (PNL). The third materials test (MT-3) was the sixth experiment in a series of thermal-hydraulic and potential deformation/rupture experiments conducted in the National Research Universal (NRU) Reactor, Chalk River, Ontario, Canada. The LOCA experiments were jointly funded by the U.S. Nuclear Regulatory Commission (NRC) and the United Kingdom Atomic Energy Authority (UKAEA) with the main objective to evaluate ballooning and rupture during active two-phase cooling at elevated temperatures. All 12 test rods in the center of the 32-rod bundle ruptured with an average peak strain of 55%.

At the request of the UKAEA, a destructive postirradiation examination (PIE) was performed on 7 of the 12 test rods. The results of this examination were presented in a previous report. Subsequently, and at the request of UKAEA, PIE was performed on three additional rods along with further examination of one of the previously examined rods. Information obtained from the PIE included cladding thickness measurements, cladding metallography, and particle size analysis of the fractured fuel pellets. This report describes the additional PIE work performed and presents the results of these examinations.

SUMMARY

The Loss-of-Coolant Accident (LOCA) Simulation Program was conducted by Pacific Northwest Laboratory to evaluate the thermal-hydraulic and mechanical deformation behavior of full-length light-water reactor (LWR) fuel bundles under LOCA conditions. The tests were designed to simulate the heatup, reflood, and quench phases of a large-break LOCA and were performed in the National Research Universal (NRU) Reactor using nuclear fission to simulate the low-level decay power typical of these conditions.

The sixth experiment in the program--Materials Test 3 (MT-3)--was jointly funded by the U.S. Nuclear Regulatory Commission (NRC) and the United Kingdom Atomic Energy Authority (UKAEA). The main objective of the MT-3 experiment was to obtain data pertinent to the licensing requirements for ballooning and blockage of fuel rod cladding. By agreement with the NRC, the test conditions were identified and selected by the UKAEA.

The results of a postirradiation examination (PIE) performed on several of the ruptured rods from the MT-3 experiment are presented in this report. Particle size analyses of the fuel from various rod sections were conducted, and metallographic specimens of the Zircaloy cladding from these sections were prepared and examined.

Metallographic examination of the Zircaloy cladding revealed that temperatures were sufficient to cause alpha grain growth and possibly an alpha to alpha-plus-beta phase transformation. Alpha grain boundaries in a number of cladding sections were lightly decorated with particles speculated as being incipient prior beta phase.

Oxidation occurred on both the inner and outer surfaces of the Zircaloy cladding, creating both zirconium oxide and an oxygen-enriched layer. The oxygen-enriched layers on the inside and outside surfaces never exceeded 2 μm in thickness. Cracking of the oxygen-enriched layer was not observed on the sections examined.

Size analysis of the fuel particles from Rod Sections 3C5, 4C5, and 4D5 revealed that one pellet from Rod Section 3C5 remained intact. The remainder of the pellets cracked into particles; most of the particles (73.12%, 59.66%, and 56.68% from Rod Sections 3C5, 4C5, and 4D5, respectively) were less than 0.233 in. (5.6 mm) and greater than 0.157 in. (4.0 mm).

SUMMARY

The Loss-of-Coolant Accident (LOCA) Simulation Program was conducted by Pacific Northwest Laboratory to evaluate the thermal hydraulic and mechanical deformation behavior of full-length light-water reactor (LWR) fuel bundles under LOCA conditions. The tests were designed to simulate the heatup, reflood, and quench phases of a large-break LOCA and were performed in the National Research Universal (NRU) reactor using nuclear fission to simulate the low-level decay power typical of these conditions.

The sixth experiment in the program—Materials Test 3 (MT-3)—was jointly funded by the U.S. Nuclear Regulatory Commission (NRC) and the United Kingdom Atomic Energy Authority (UKAEA). The main objective of the MT-3 experiment was to obtain data pertinent to the licensing requirements for ballooning and blockage of fuel rod cladding. By agreement with the NRC, the test conditions were identified and selected by the UKAEA.

The results of a postirradiation examination (PIE) performed on several of the ruptured rods from the MT-3 experiment are presented in this report. Particle size analyses of the fuel from various rod sections were conducted, and metallographic specimens of the Zircaloy cladding from these sections were prepared and examined.

Metallographic examination of the Zircaloy cladding revealed that temperatures were sufficient to cause alpha grain growth and possibly an alpha to alpha-plus-beta phase transformation. Alpha grain boundaries in a number of cladding sections were lightly decorated with particles speculated as being incipient prior beta phase.

Oxidation occurred on both the inner and outer surfaces of the Zircaloy cladding, creating both zirconium oxide and an oxygen-enriched layer. The oxygen-enriched layer on the inside and outside surfaces never exceeded 2 µm in thickness. Cracking of the oxygen-enriched layer was not observed on the sections examined.

Sizing analysis of the fuel particles from Rod Sections 205, 405, and 408 revealed that one pellet from Rod Section 205 remained intact. The remainder of the pellets cracked into particles; most of the particles (73.12%, 59.68%, and 55.83% from Rod Sections 205, 405, and 408, respectively) were less than 0.263 in. (6.68 mm) and greater than 0.157 in. (4.0 mm).

CONTENTS

FIGURES

TABLES

INTRODUCTION

A series of in-reactor experiments were conducted by Pacific Northwest Laboratory (PNL)[a] using full-length 32-rod pressurized water reactor (PWR) fuel bundles as part of the Loss-of-Coolant Accident (LOCA) Simulation Program (Hann 1979). The third materials test (MT-3) was the sixth in the series of thermal-hydraulic and materials deformation/rupture experiments conducted in the National Research Universal (NRU) Reactor at the Chalk River Nuclear Laboratory (CRNL),[b] Chalk River, Ontario, Canada. The experiment was jointly funded by the U.S. Nuclear Regulatory Commission (NRC) and the United Kingdom Atomic Energy Authority (UKAEA).

The main objective of MT-3 was to evaluate the ballooning and rupture behavior of the cladding during active two-phase cooling in the temperature range from 1400 to 1500°F (1030 to 1090K). The 32-rod assembly contained 12 test rods in the center of the assembly (Table 1); 7 of the 12 rods were selected for destructive postirradiation examination (PIE). The results of the examination were presented in an earlier report (Rausch 1984).

Subsequently, additional destructive PIE was performed on three additional rods and the ruptured area of Rod 2C, which had been examined in the first campaign. The rods were sectioned for metallographic examination and fuel fragment size analysis. A detailed metallographic examination of the cladding was performed around the ruptured region of each rod, and cladding thickness measurements were made around the circumference of the cladding cross sections. Specimen MET-4 from Rod Section 2C5, previously examined for wall and oxide thickness measurements, was re-examined.

The PIE is described and the results of the examination are presented in this report.

TABLE 1. MT-3 Fuel Rod Parameters

Cladding Material	Zircaloy-4
Cladding Outside Diameter (OD)	0.379 in. (0.963 cm)
Cladding Inside Diameter (ID)	0.331 in. (0.841 cm)
Pitch (rod to rod)	0.502 in. (1.275 cm)
Fuel Pellet (OD)	0.325 in. (0.825 cm)
Fuel Pellet Length	0.375 in. (0.953 cm)
Active Fueled Length	144 in. (365.75 cm)
Total Shroud Length	170.125 in. (423.1 cm)
Helium Pressurization	550 psig (3.8 MPa)
Fuel Enrichment	2.93% ^{235}U

(a) Operated for the U.S. Department of Energy (DOE) by Battelle Memorial Institute.
(b) Operated by Atomic Energy of Canada, Ltd. (AECL).

INTRODUCTION

A series of in-reactor experiments were conducted by Pacific Northwest Laboratory (PNL)[a] using full-length 32-rod pressurized water reactor (PWR) fuel bundles as part of the Loss-of-Coolant Accident (LOCA) Simulation Program (Hann 1979). The third materials test (MT-3) was the sixth in the series of thermal-hydraulic and materials deformation/rupture experiments conducted in the National Research Universal (NRU) reactor at the Chalk River Nuclear Laboratory (CRNL),[b] Chalk River, Ontario, Canada. The experiment was jointly funded by the U.S. Nuclear Regulatory Commission (NRC) and the United Kingdom Atomic Energy Authority (UKAEA).

The main objective of MT-3 was to evaluate the ballooning and rupture behavior of the cladding during active two-phase cooling in the temperature range from 1400 to 1600°F (1030 to 1090K). The 32-rod assembly contained 12 test rods in the center of the assembly (Table 1). Two of the 12 rods were selected for destructive postirradiation examination (PIE). The results of the examination were presented in an earlier report (Rausch 1984).

Subsequently, additional destructive PIE was performed on three additional rods and the ruptured area of Rod [illegible] which had been examined in the first campaign. The rods were sectioned for metallographic examination and fuel fragment size analysis. A detailed metallographic examination of the cladding was performed around the ruptured region of each rod, and cladding thickness measurements were made around the circumference of the cladding cross sections. Specimen MT-3 from Rod Section [illegible], previously examined for wall and oxide thickness measurements, was re-examined.

The PIE is described and the results of the examination are presented in this report.

TABLE 1. MT-3 Fuel Rod Parameters

Cladding Material	Zircaloy-4
Cladding Outside Diameter (OD)	0.379 in. (0.963 cm)
Cladding Inside Diameter (ID)	0.331 in. (0.841 cm)
Pitch (rod to rod)	0.502 in. (1.275 cm)
Fuel Pellet (OD)	0.325 in. (0.826 cm)
Fuel Pellet Length	[illegible]
Active Fueled Length	144 in. (365.76 cm)
Total Shroud Length	170.125 in. (432.1 cm)
Helium Pressurization	550 psig (3.8 MPa)
Fuel Enrichment	2.93% ^{235}U

(a) Operated for the U.S. Department of Energy (DOE) by Battelle Memorial Institute.
(b) Operated by Atomic Energy of Canada, Ltd. (AECL).

DESCRIPTION OF POSTIRRADIATION EXAMINATION

Three rods (3C, 4C, and 4D) were selected for detailed examination of the cladding and size analysis of the fragmented fuel. Sections approximately 18 in. long, including the ruptured region, were cut from each rod in the universal cells and transported to the hot cells for detailed PIE. In addition, the section of Rod 2C containing the ruptured region and a metallographic sample (MET-4) from Rod Section 2C5 that had been previously examined were obtained from storage for examination.

The locations of the metallographic samples were determined from photographs and reference markings scribed along the length of the rod during the DERM (Disassembly, Examination, Reassembly Machine) analysis (Mohr et al. 1983). The rupture centerline was also used to locate additional areas of interest. The 18-in. long sections were dissected into 1-in. long samples for metallographic preparation and examination of the cladding cross sections. Details of the sample sectioning, mounting, and preparation procedure were outlined in a previous report (Rausch 1984). The sample cross sections that were examined and their axial locations are identified in Table 2.

Cladding wall thickness measurements were taken around the circumference of each sample cross section at regular intervals (cord of 0.040 in. or 1.02 mm) using the microscope viewing screen at a magnification of 200X. The Zircaloy cladding sections were anodized in Picklesimer's solution (Picklesimer 1957) to reveal possible beta phase. The cladding sections were then metallurgically examined and photographed at high magnifications. The appearance of the grain structure at different locations around the circumference was noted. The thicknesses of the zirconium oxide and the oxygen-enriched layer on the outer and inner surfaces of the cladding were measured.

Particle size analysis was performed on the fuel from Rod Sections 3C5, 4C5, and 4D5. Six standard 8-in. (203-mm) diameter sieves were stacked on a portable sieve shaker. The mesh sizes were 0.223 in. (5.60 mm), 0.157 in. (4.00 mm), 0.111 in. (2.80 mm), 0.0787 in. (2.00 mm), 0.0394 in. (1.00 mm), and 0.0117 in. (300 μm). After approximately 10 min of shaking, the fuel fragments in each sieve were poured onto a tarred tissue paper, which was then weighed to 0.001 gram on a balance in the hot cell.

TABLE 2. Axial Locations of Cladding Cross Sections

MT-3 Rod	Designation[a]	Position[b]
3C	3C5-1	98
3C	3C5-2	99
3C	3C5-3	100
3C	3C5-4	101
3C	3C5-5	102
3C	3C5-6	103
3C	3C5-7	104
3C	3C5-8	105
3C	3C5-9	106
3C	3C5-10	107
4C	4C5-1	99.5
4C	4C5-2	100.5
4C	4C5-3	101.5
4C	4C5-4	102.5
4C	4C5-5	103.5
4C	4C5-6	104.5
4C	4C5-7	105.5
4C	4C5-8	106.5
4C	4C5-9	107.5
4D	4D5-1	98
4D	4D5-2	99
4D	4D5-3	100
4D	4D5-4	101
4D	4D5-5	102
4D	4D5-6	103
4D	4D5-7	104
4D	4D5-8	105
4D	4D5-9	106
4D	4D5-10	107
2C	2C5-7	103
2C	2C5-4	98

(a) For example, 3C5-1 = Rod 3C from Assembly 5 (MT-3 was the sixth test in the NRU LOCA Program; however, two of the earlier tests used the same assembly), Metallographic Section 1.

(b) Elevation in inches from the bottom of the rod.

POSTIRRADIATION EXAMINATION RESULTS

The 1-in. long metallurgical sections were mounted, prepared, and photographed for detailed examination of the cladding cross section. Observations of the microstructure along with zirconium oxide and oxygen-enriched layer thickness measurements on the inner and outer surfaces of the cladding were made at different locations around the circumference. Reproductions were made from the photographs, which depict the contour of the cladding. The reproductions, presented in Figures 1 through 16, were not of adequate quality to show the grain structure or the zirconium oxide layer; therefore, the features of interest are noted on the figures.

The thicknesses of the oxygen-enriched layers on the specimens are presented in Table 3. The layers varied in thickness from 0.5 to 2.0 μm on the inner and outer surfaces of all cladding sections except 3C5-1, 3C5-9, 4C5-8, and 4C5-9, where no oxygen-enriched layer was visible. Cracking of the oxygen-enriched layer was not observed on any of the cladding sections. Figure 17 is a representative photomicrograph showing the zirconium oxide and oxygen-enriched layers on the inner and outer surfaces of the cladding.

An examination of the cladding microstructure indicated that the cladding had reached temperatures that caused alpha grain growth and possibly transformed the structure of certain cladding sections to alpha plus beta. Alpha grain boundaries of a number of Zircaloy cladding sections examined were found to be lightly decorated with a small amount of a precipitated phase as noted in Figure 18. The precipitated phase is speculated to be incipient prior beta phase. A photomicrograph showing alpha grain boundaries with a small amount of incipient prior beta phase, for comparison, can be found in a previous report (Chung, Garde, and Kassner 1975). Incipient prior beta phase precipitated at alpha grain boundaries was readily observed in a number of the Zircaloy cladding sections examined; namely, Rod Sections 4C5-4, 4D5-2, 4D5-3, 4D5-4, 4D5-5, and 4D5-6. The alpha to alpha-plus-beta phase transformation temperature of Zircaloy-4 has been reported to be 809°C (Chung, Garde, and Kassner 1975). Because of the minuteness of the prior beta phase, the cladding sections with the incipient prior beta are estimated to have attained temperatures slightly higher than the phase transformation temperature.

To further verify that the cladding sections did indeed approach the alpha to alpha-plus-beta phase transformation temperature, it is possible to compare the observed zirconium oxide layer thickness of the Zircaloy-4 cladding sections examined with thicknesses formed at known temperatures and time. Studies of Zircaloy-2 oxidation were performed at various time/temperature combinations (Donaldson and Evans 1980). The rate at which the zirconium oxide layer grew was reported to follow a parabolic rate equation of the form:

$$\varepsilon = kt^{1/2} \qquad (1)$$

where ε = the thickness of the zirconium oxide layer
t = the time at elevated temperature
k = the parabolic rate constant.

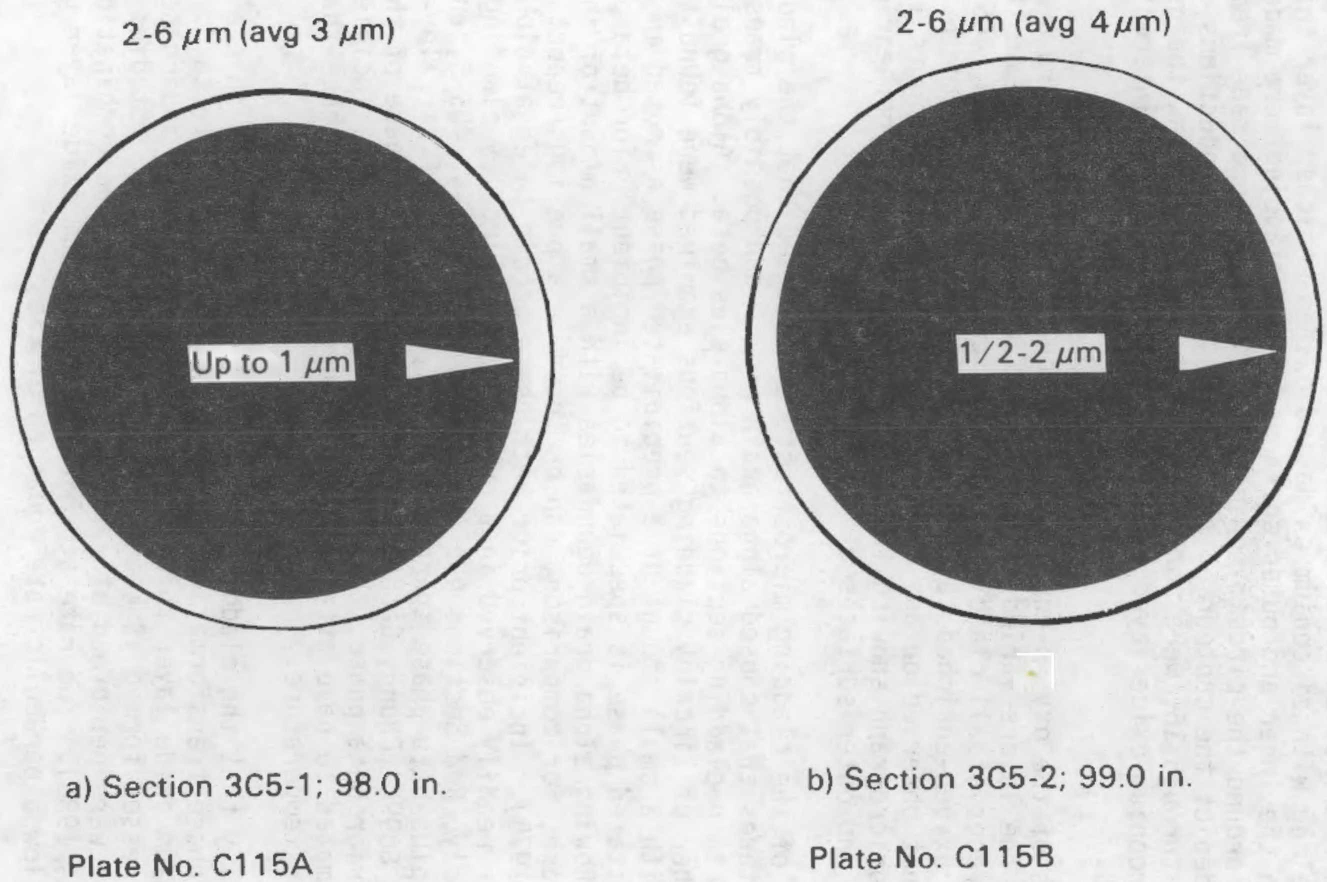

FIGURE 1. Zirconium Oxide Thicknesses on Outer and Inner Surfaces of Rod Sections 3C5-1 and 3C5-2 (white triangles indicate the reference point for wall thickness measurements)

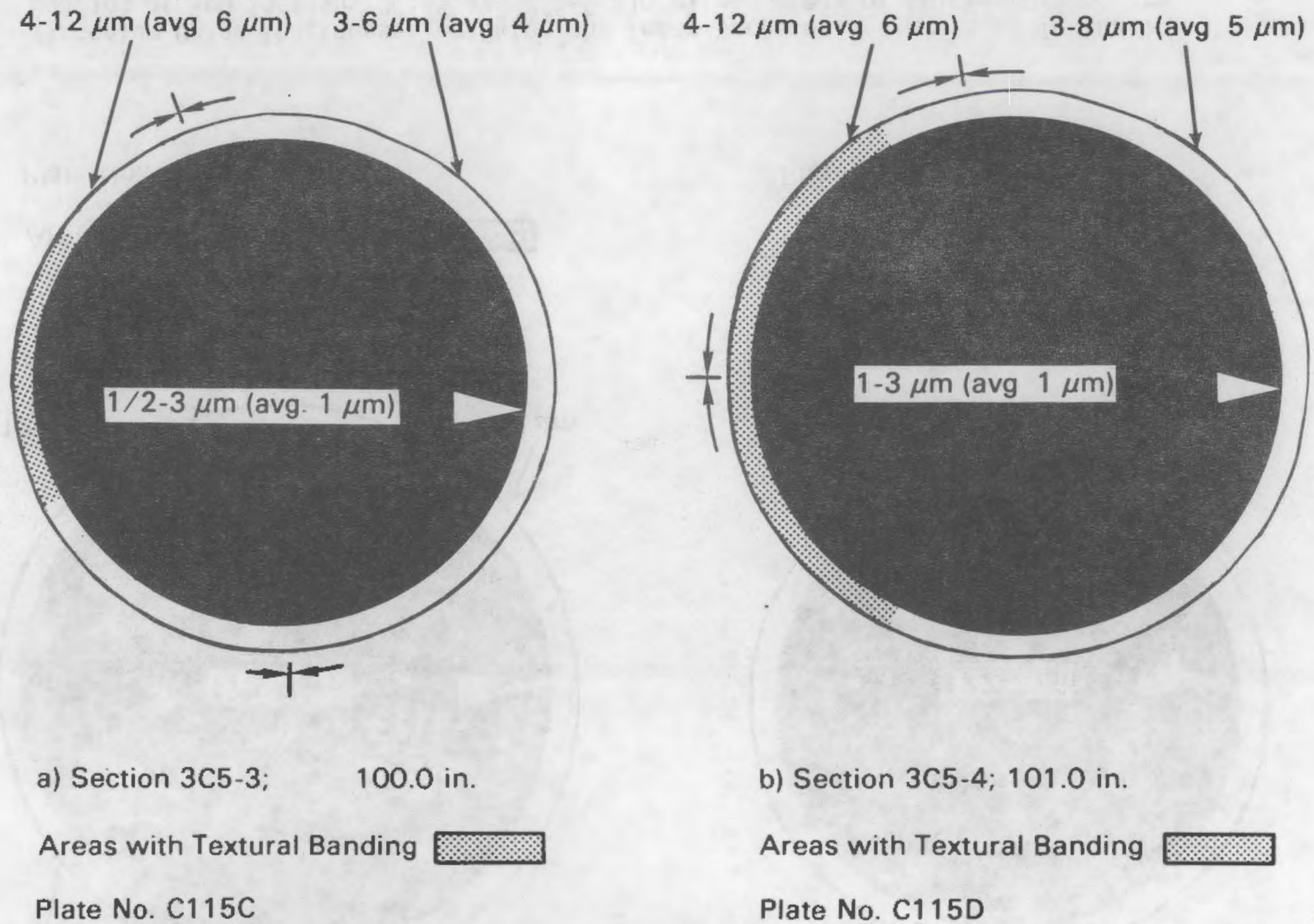

FIGURE 2. Zirconium Oxide Thicknesses on Outer and Inner Surfaces and Areas of Textural Banding of Rod Sections 3C5-3 and 3C5-4 (white triangles indicate the reference point for wall thickness measurements)

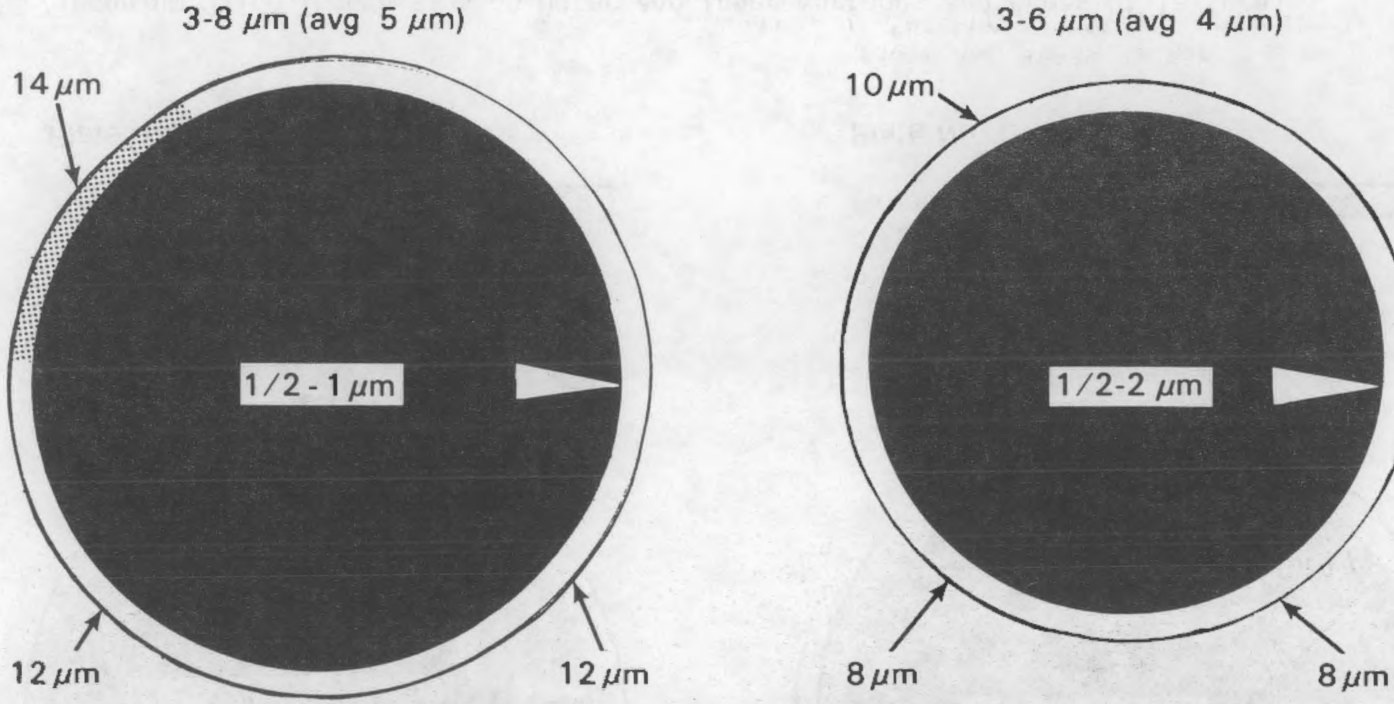

a) Section 3C5-5; 102.0 in.

b) Section 3C5-6; 103.0 in.

Areas with Textural Banding

Plate No. C115E

Plate No. C115F

FIGURE 3. Zirconium Oxide Thicknesses on Outer and Inner Surfaces and Areas of Textural Banding of Rod Sections 3C5-5 and 3C5-6 (localized areas of thicker oxides are indicated; white triangles indicate the reference point for wall thickness measurements)

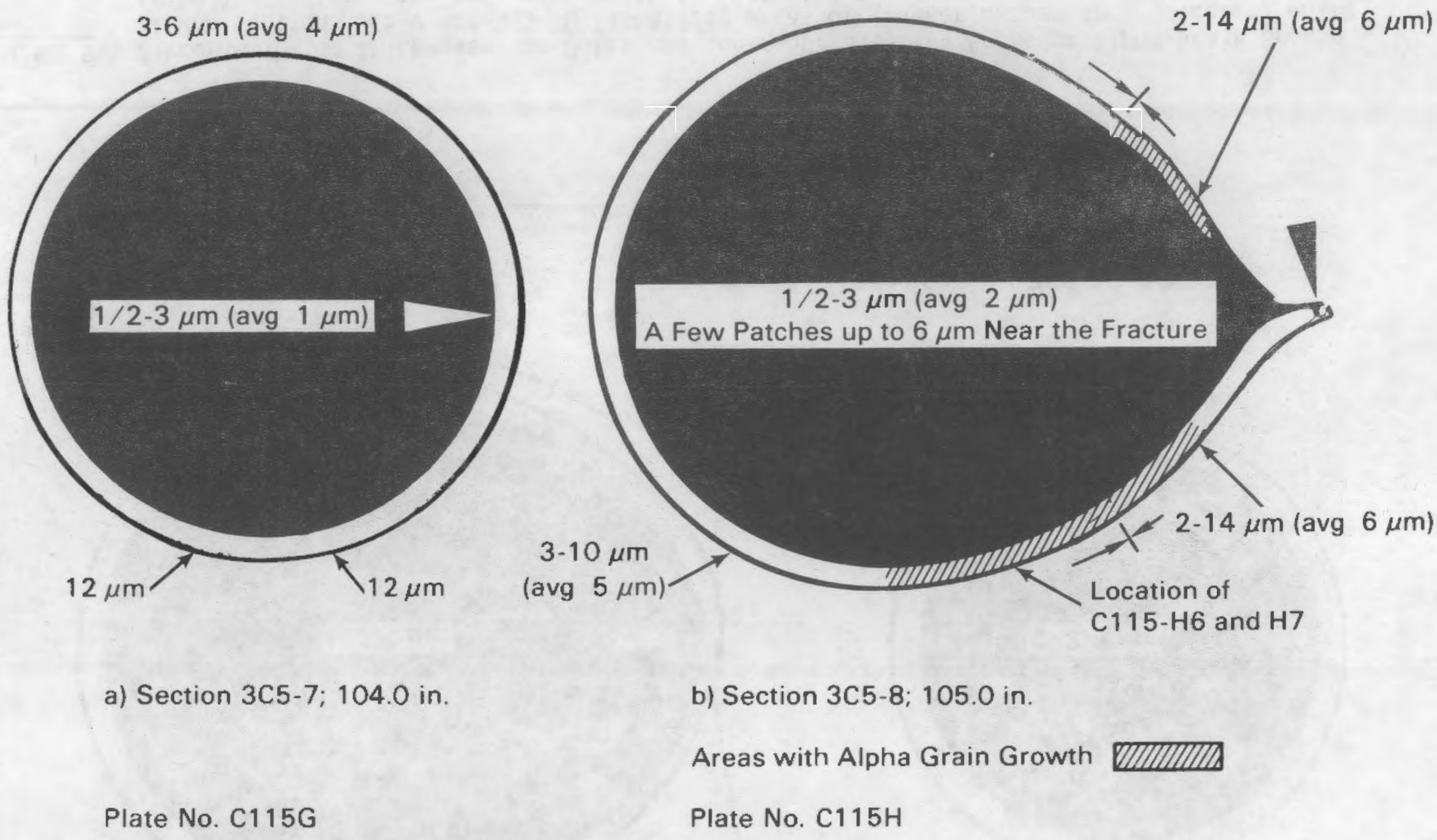

FIGURE 4. Zirconium Oxide Thicknesses on Outer and Inner Surfaces and Areas of Alpha Grain Growth of Rod Sections 3C5-7 and 3C5-8 (localized areas of thicker oxides are indicated; triangles indicate the reference point for wall thickness measurements)

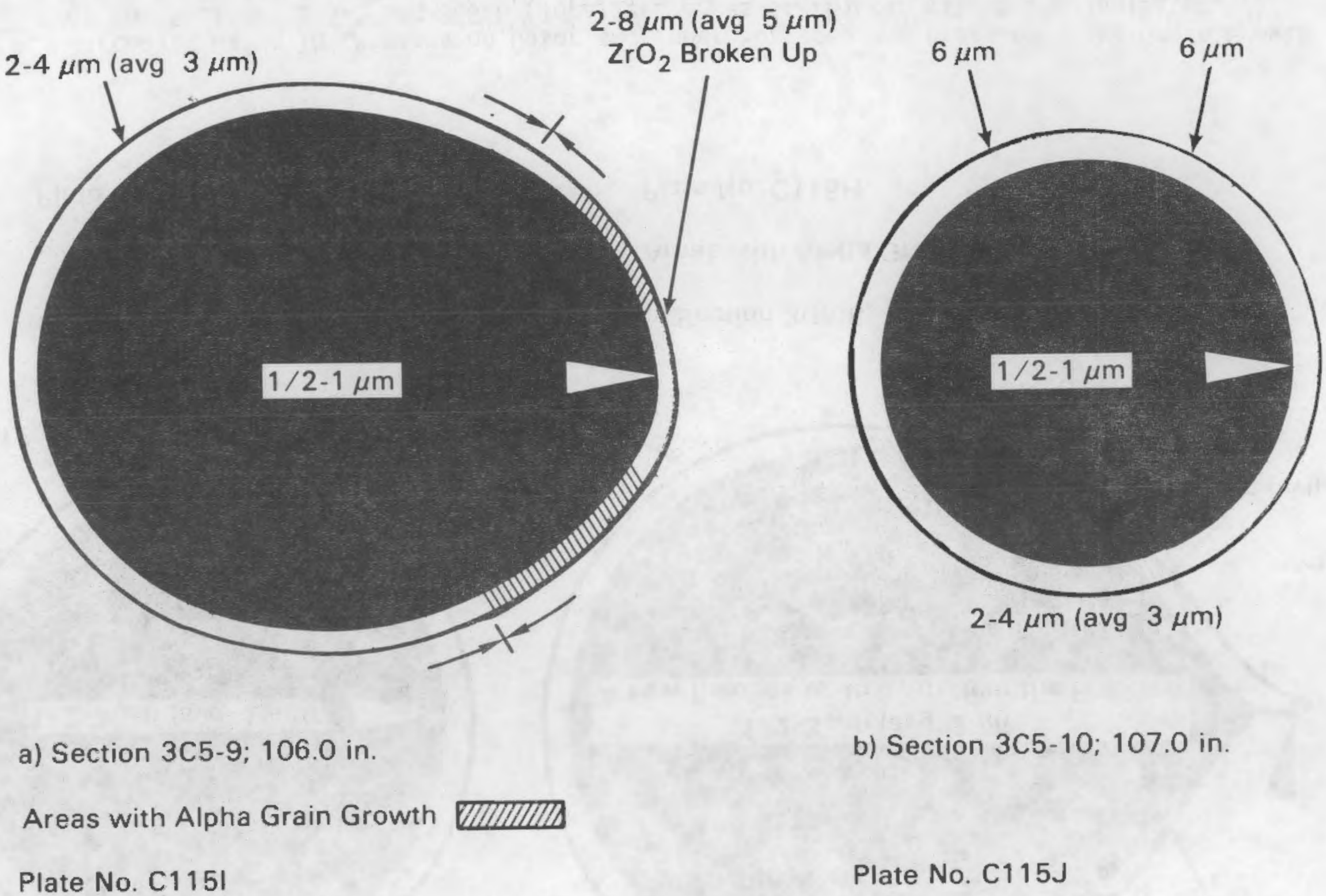

FIGURE 5. Zirconium Oxide Thicknesses on Outer and Inner Surfaces and Areas of Alpha Grain Growth of Rod Sections 3C5-9 and 3C5-10 (localized areas of thicker oxides are indicated; white triangles indicate the reference point for wall thickness measurements)

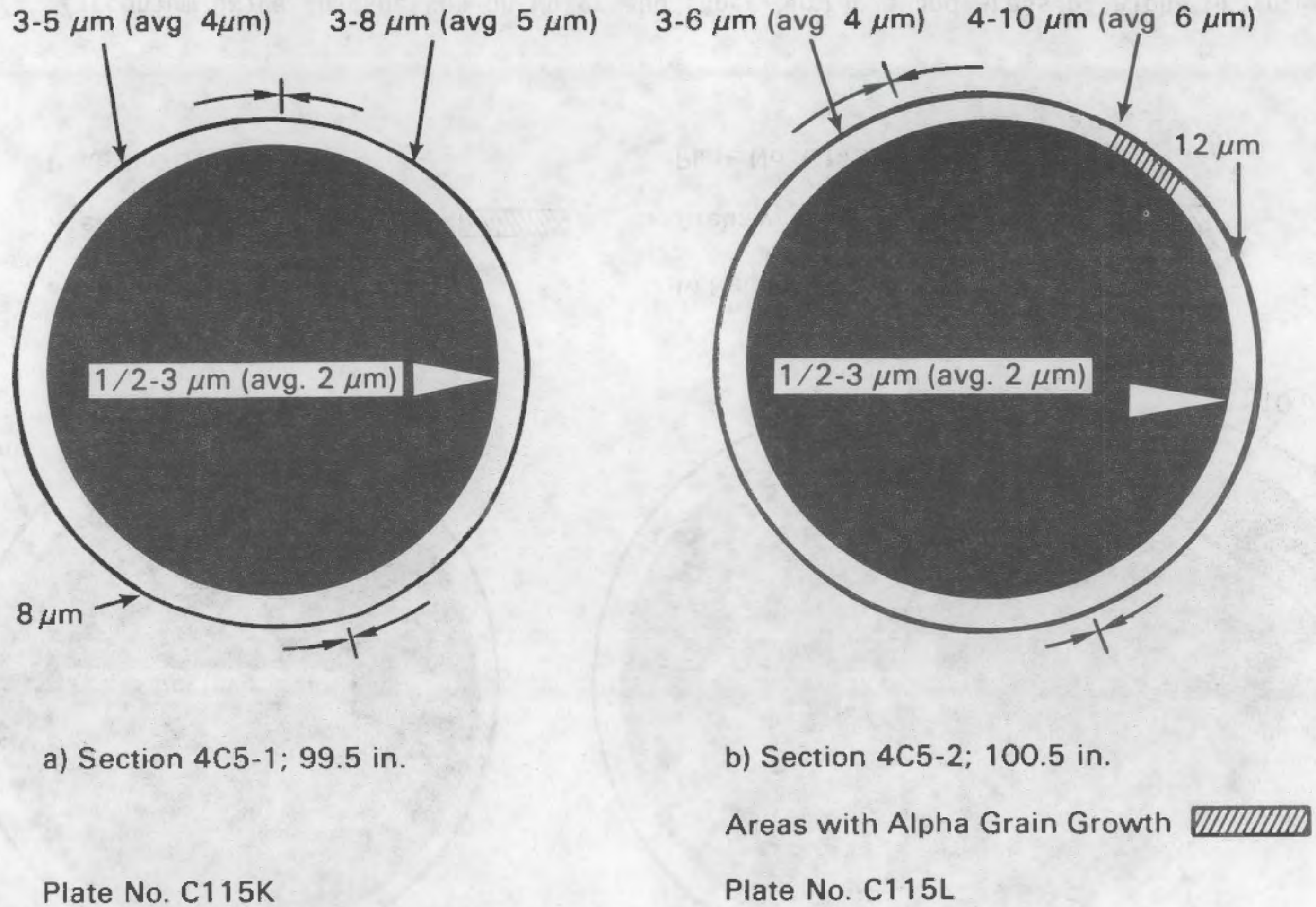

FIGURE 6. Zirconium Oxide Thicknesses on Outer and Inner Surfaces and Areas of Alpha Grain Growth of Rod Sections 4C5-1 and 4C5-2 (localized areas of thicker oxides are indicated; white triangles indicate the reference point for wall thickness measurements)

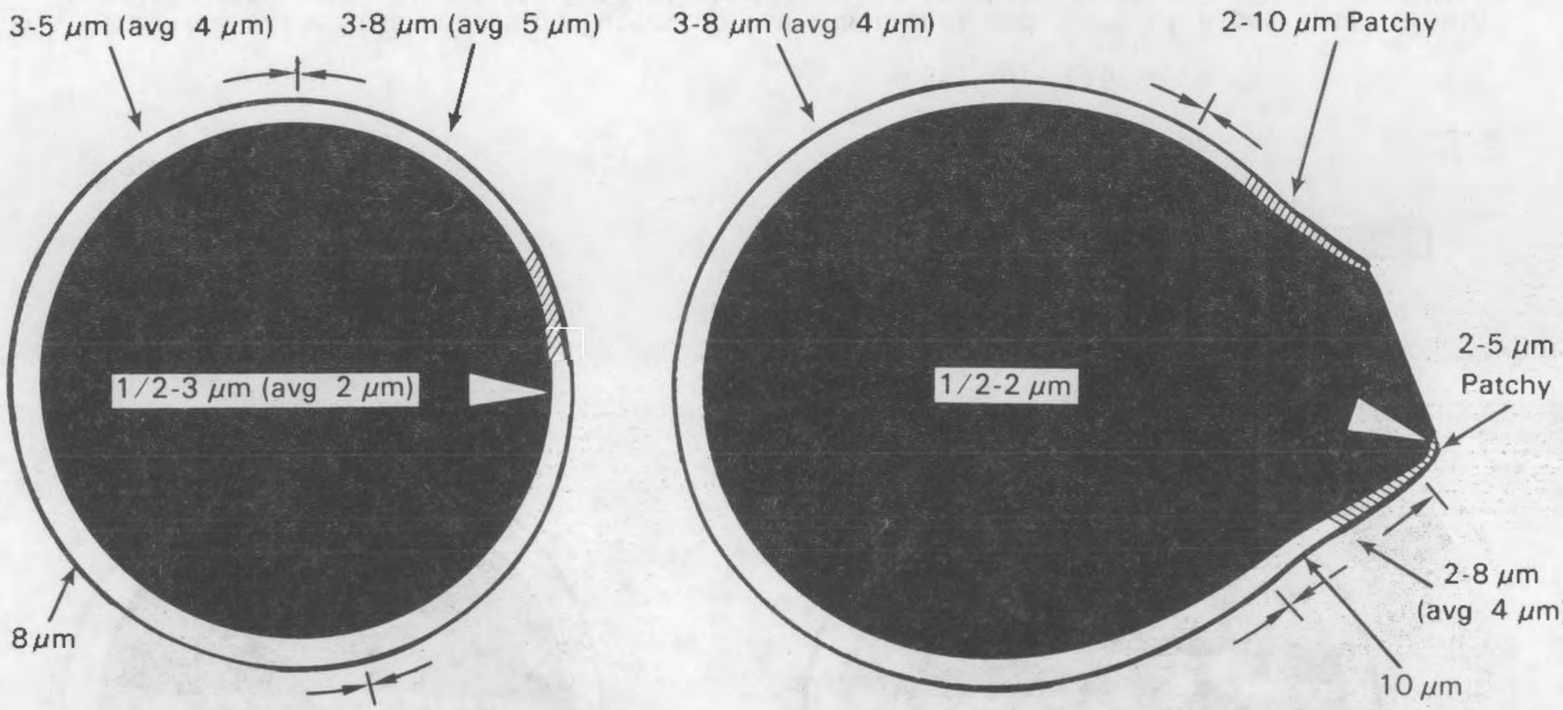

a) Section 4C5-3; 101.5 in.

Areas with Alpha Grain Growth

Plate No. C115M

b) Section 4C5-4; 102.5 in.

Areas with Alpha Grain Growth

Plate No. C115N

FIGURE 7. Zirconium Oxide Thicknesses on Outer and Inner Surfaces and Areas of Alpha Grain Growth of Rod Sections 4C5-3 and 4C5-4 (localized areas of thicker oxides are indicated; white triangles indicate the reference point for wall thickness measurements)

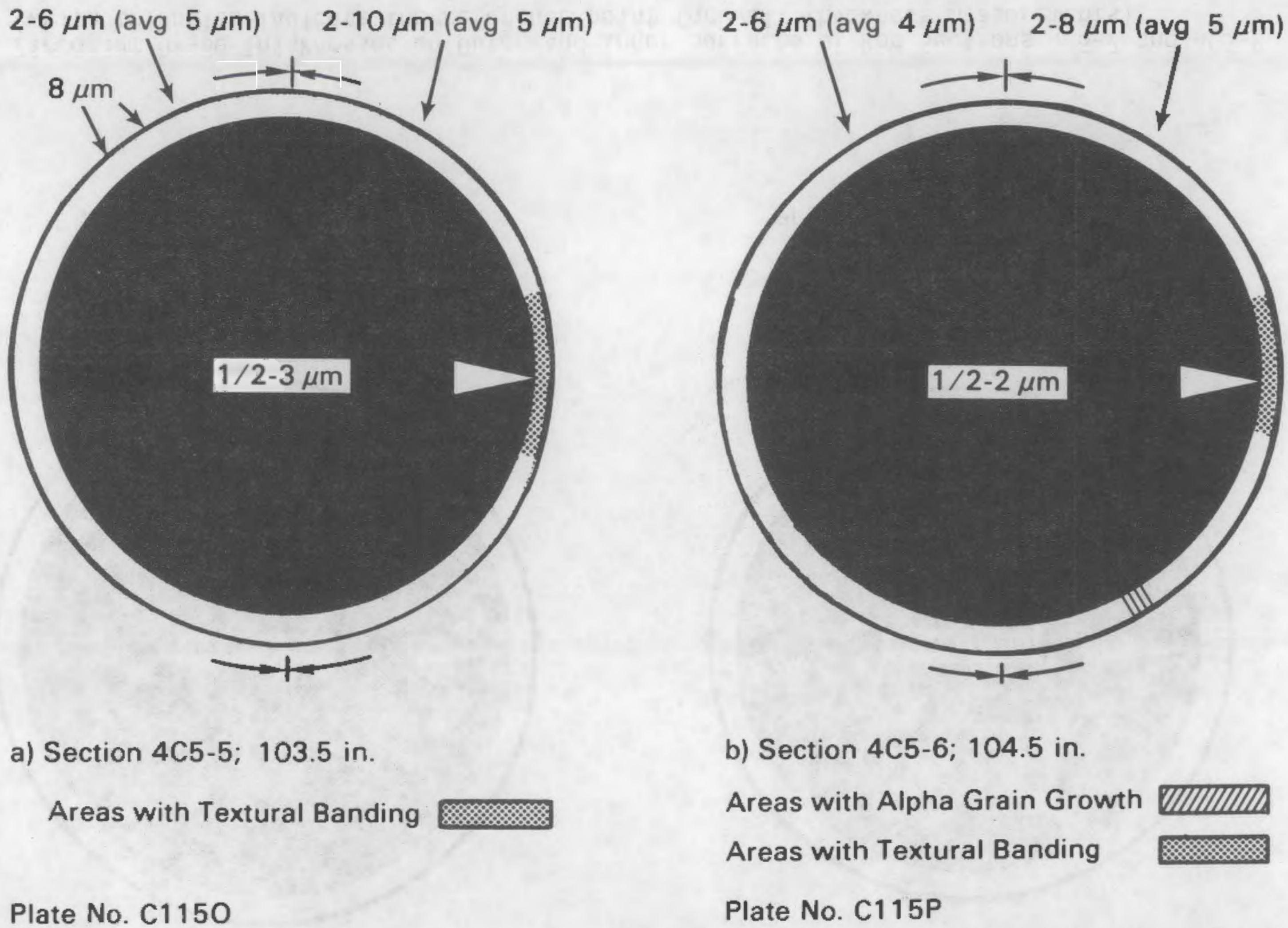

FIGURE 8. Zirconium Oxide Thicknesses on Outer and Inner Surfaces, Areas of Alpha Grain Growth, and Textural Banding of Rod Sections 4C5-5 and 4C5-6 (localized areas of thicker oxides are indicated; white triangles indicate the reference point for wall thickness measurements)

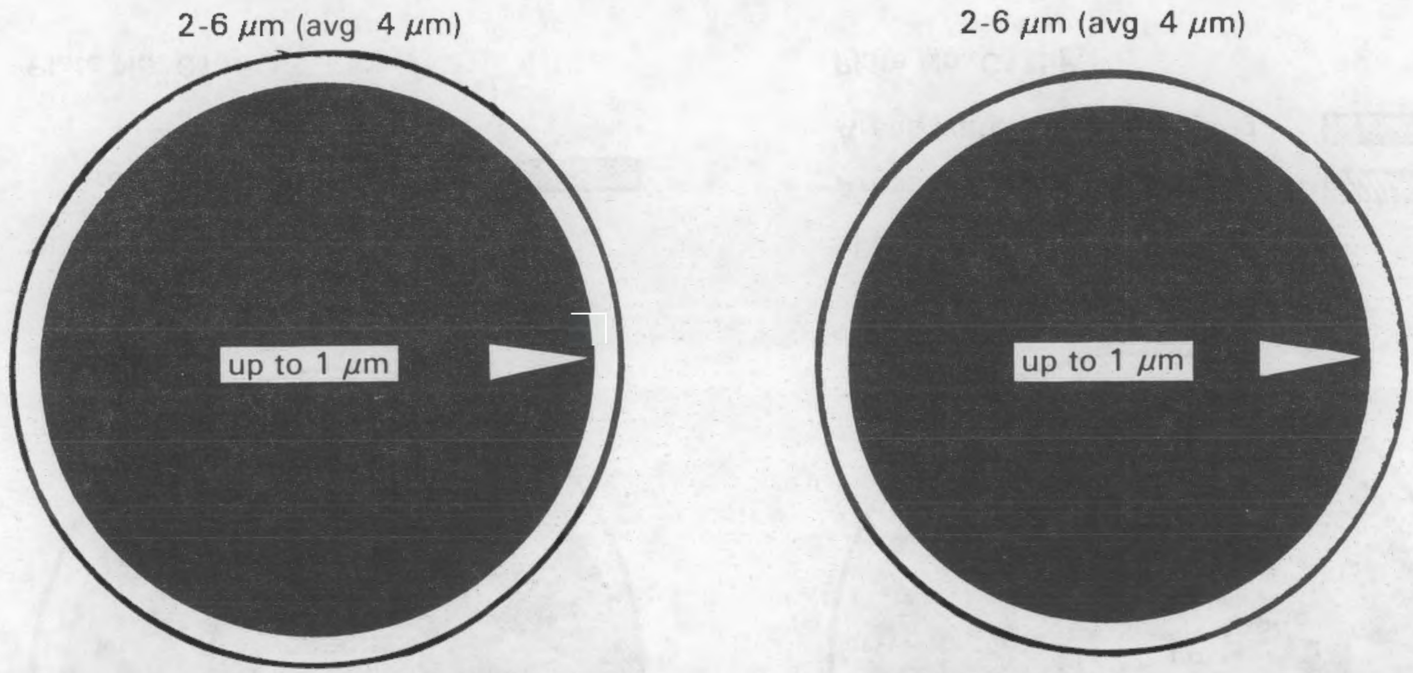

a) Section 4C5-7; 105.5 in.

Plate No. C115R

b) Section 4C5-8; 106.5 in.

Plate No. C115S

FIGURE 9. Zirconium Oxide Thicknesses on Outer and Inner Surfaces of Rod Sections 4C5-7 and 4C5-8 (white triangles indicate the reference point for wall thickness measurements)

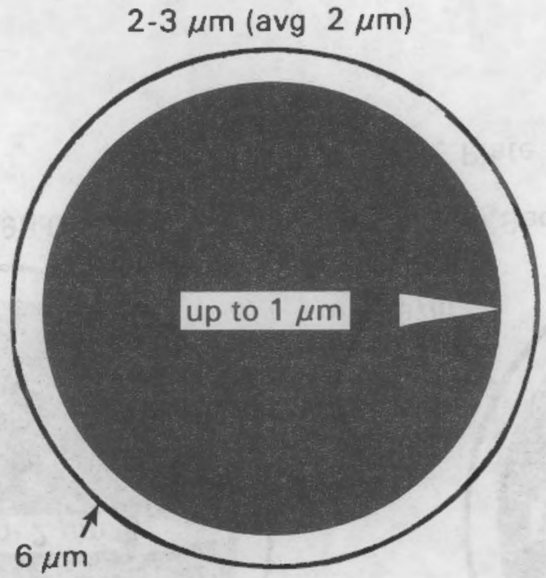

a) Section 4C5-9; 107.5 in.

Plate No. C115T

FIGURE 10. Zirconium Oxide Thicknesses on Outer and Inner Surfaces of Rod Section 4C5-9 (localized area of thicker oxide is indicated; white triangle indicates the reference point for wall thickness measurements)

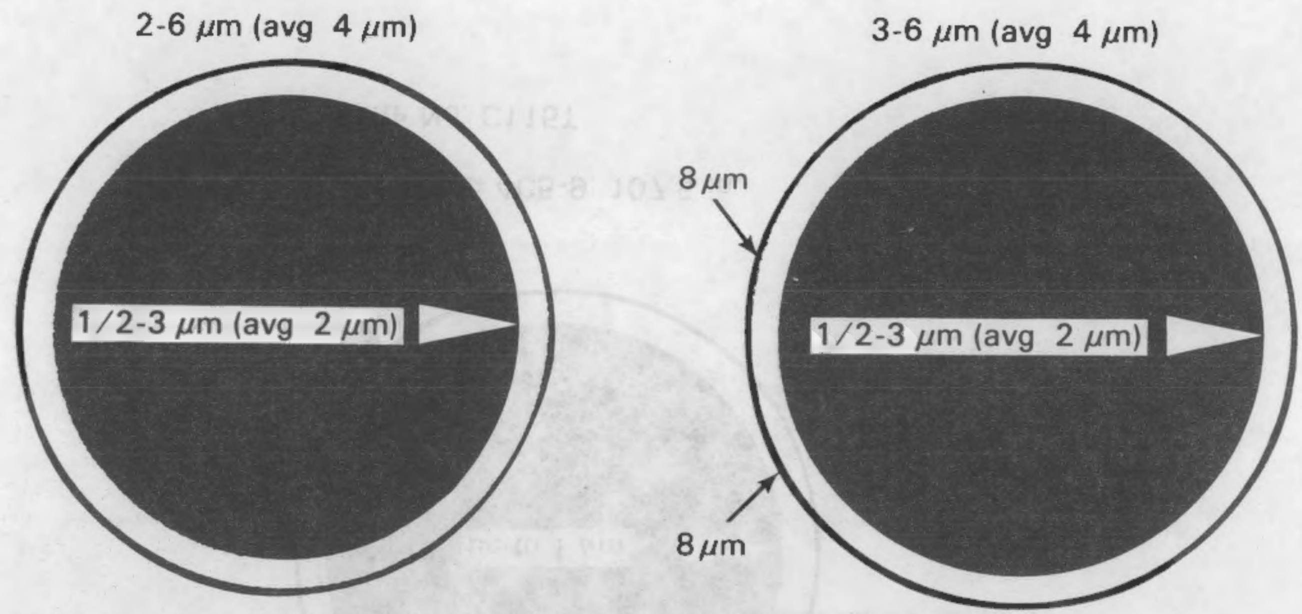

a) Section 4D5-1; 98.0 in.

Plate No. C116A

b) Section 4D5-2; 99.0 in.

Plate No. C116B

FIGURE 11. Zirconium Oxide Thicknesses on Outer and Inner Surfaces of Rod Sections 4D5-1 and 4D5-2 (localized areas of thicker oxides are indicated; white triangles indicate the reference point for wall thickness measurements)

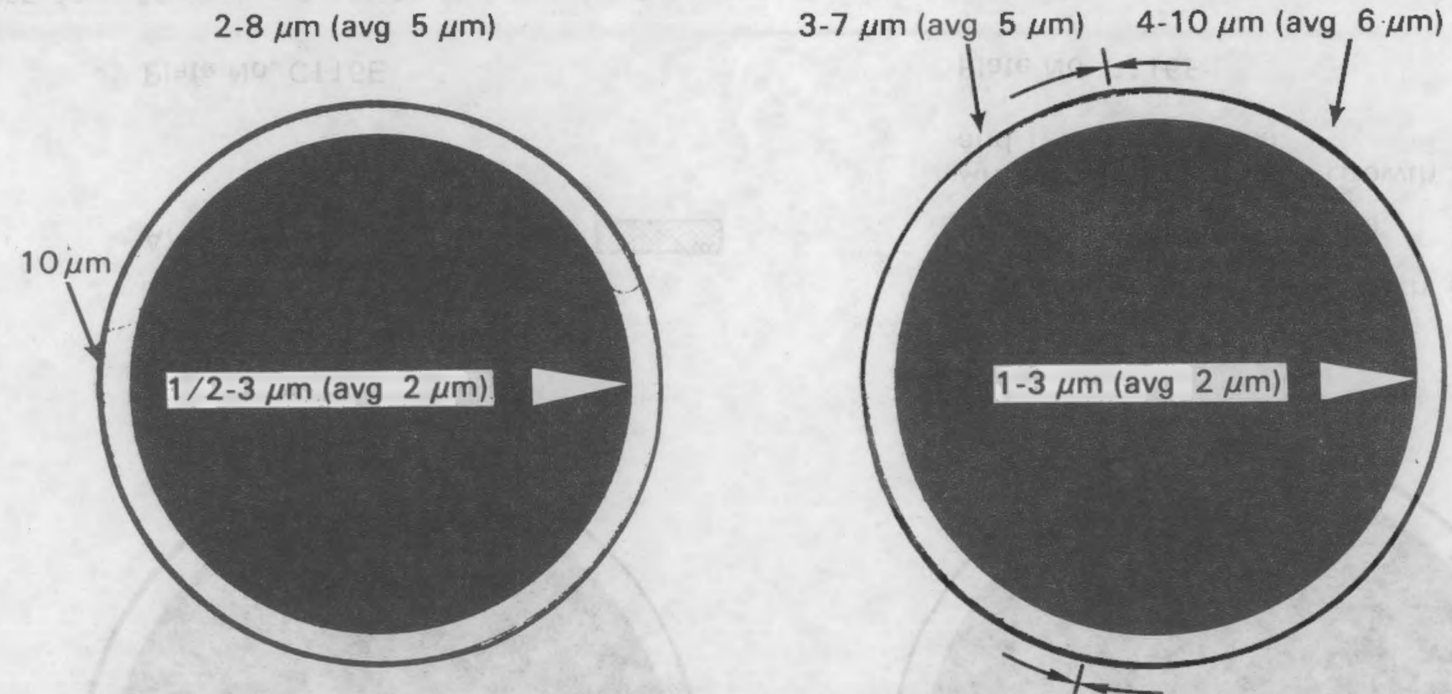

a) Section 4D5-3; 100.0 in.

Plate No. C116C

b) Section 4D5-4; 101.0 in.

Plate No. C116D

FIGURE 12. Zirconium Oxide Thicknesses on Outer and Inner Surfaces of Rod Sections 4D5-3 and 4D5-4 (localized area of thicker oxide is indicated; white triangles indicate the reference point for wall thickness measurements)

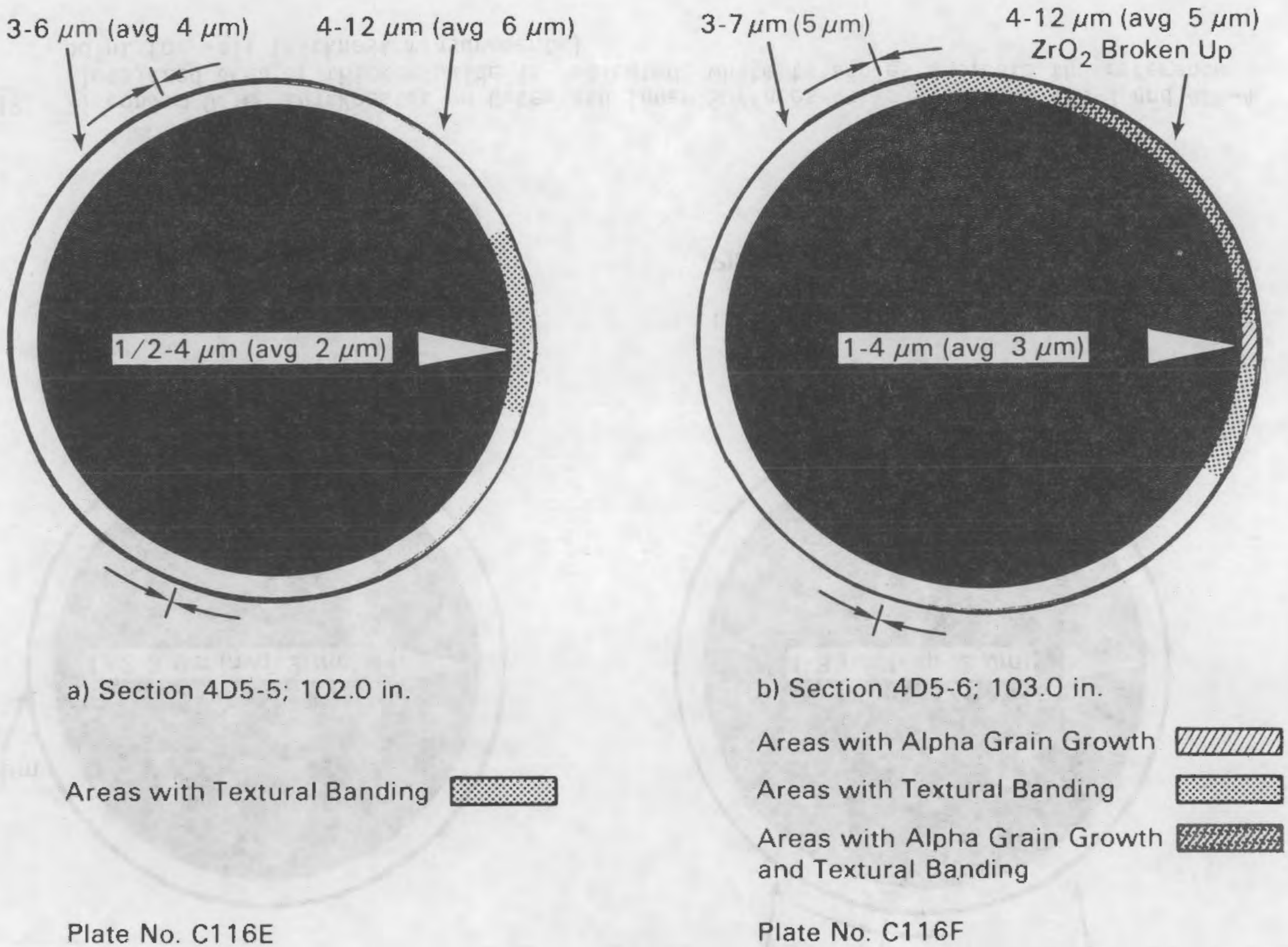

FIGURE 13. Zirconium Oxide Thicknesses on Outer and Inner Surfaces, Areas of Alpha Grain Growth, Textural Banding, and Combined Alpha Grain Growth and Textural Banding of Rod Sections 4D5-5 and 4D5-6 (white triangles indicate the reference point for wall thickness measurements)

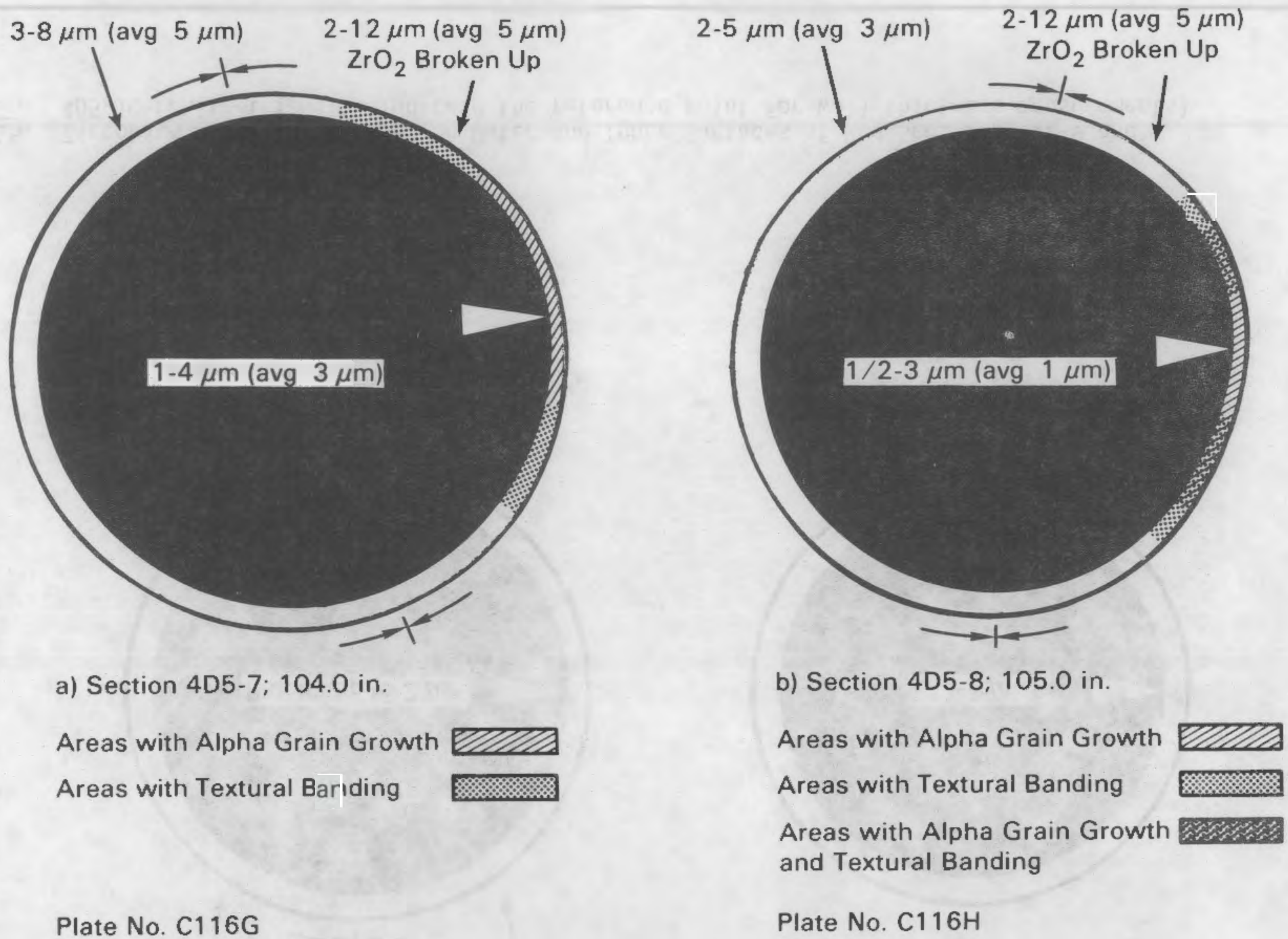

FIGURE 14. Zirconium Oxide Thicknesses on Outer and Inner Surfaces, Areas of Alpha Grain Growth, Textural Banding, and Combined Alpha Grain Growth and Textural Banding of Rod Sections 4D5-7 and 4D5-8 (white triangles indicate the reference point for wall thickness measurements)

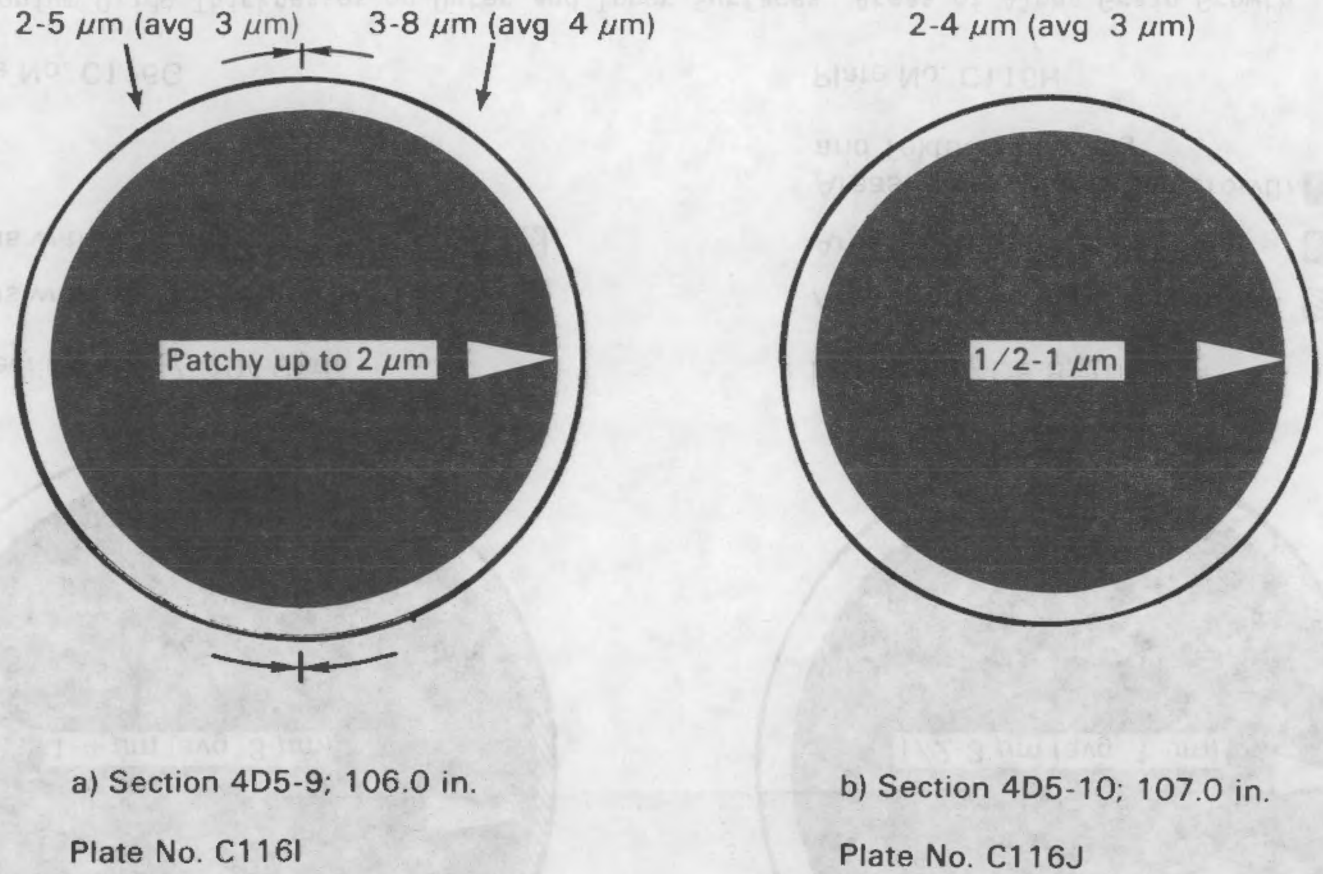

FIGURE 15. Zirconium Oxide Thicknesses on Outer and Inner Surfaces of Rod Sections 4D5-9 and 4D5-10 (white triangles indicate the reference point for wall thickness measurements)

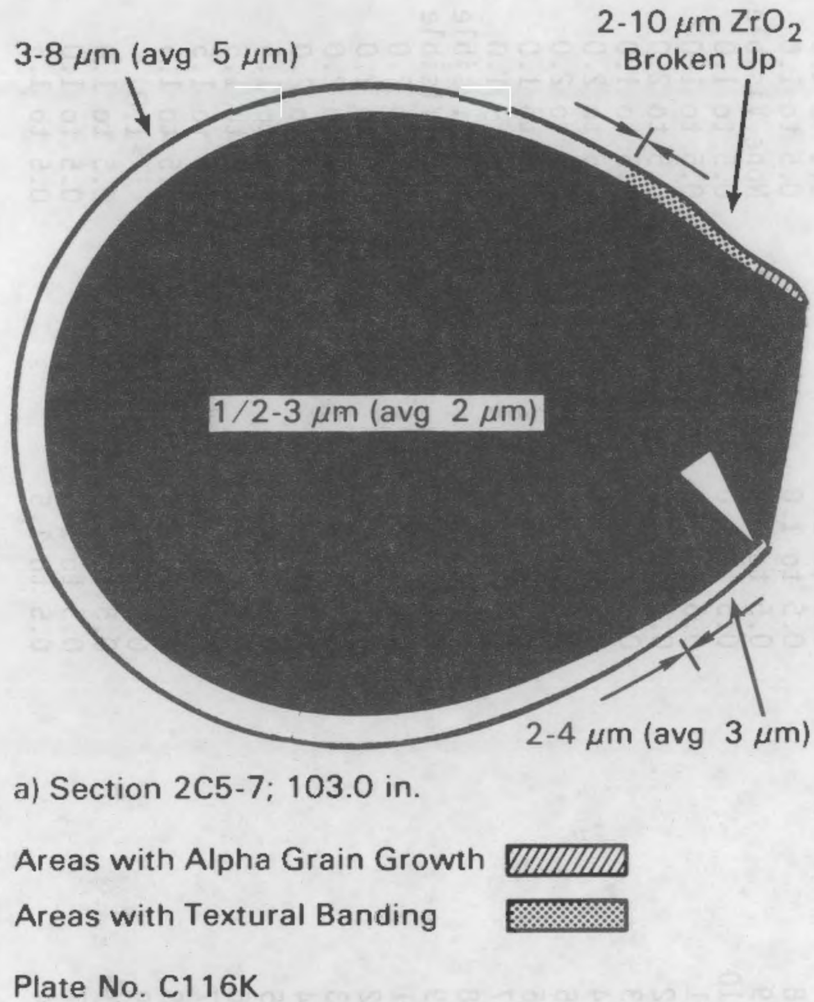

FIGURE 16. Zirconium Oxide Thicknesses on Outer and Inner Surfaces, Areas of Alpha Grain Growth, and Textural Banding of Rod Section 2C5-7 (white triangle indicates the reference point for wall thickness measurements)

TABLE 3. Thickness of Oxygen-Enriched Layers of Zircaloy Cladding

Rod Section Identity	Thickness of Oxygen-Enriched Layer, μm Outer Surface	Inner Surface
3C5-1	None Visible	None Visible
3C5-2	0.5 to 2.0	None Visible
3C5-3	1.0 to 2.0	0.5 to 1.5
3C5-4	0.5 to 2.0	0.5 to 1.5
3C5-5	0.5 to 2.0	0.5 to 1.5
3C5-6	0.5 to 2.0	0.5 to 1.5
3C5-7	0.5 to 1.5	0.5 to 1.0
3C5-8	0.5 to 1.0	0.5 to 1.0
3C5-9	0.5 to 1.0	None Visible
3C5-10	0.5 to 1.0	0.5 to 1.0
4C5-1	0.5 to 1.0	0.5 to 1.0
4C5-2	0.5 to 2.0	0.5 to 2.0
4C5-3	0.5 to 1.5	0.5 to 1.0
4C5-4	0.5 to 2.0	0.5 to 2.0
4C5-5	0.5 to 2.0	0.5 to 2.0
4C5-6	0.5 to 1.5	0.5 to 1.0
4C5-7	0.5 to 1.0	0.5 to 1.0
4C5-8	0.5	None Visible
4C5-9	0.5 to 1.0	None Visible
4D5-1	0.5 to 2.0	0.5 to 2.0
4D5-2	0.5 to 2.0	0.5 to 2.0
4D5-3	0.5 to 2.0	0.5 to 2.0
4D5-4	0.5 to 2.0	0.5 to 2.0
4D5-5	0.5 to 2.0	0.5 to 1.5
4D5-6	0.5 to 2.0	0.5 to 1.5
4D5-7	1.0 to 2.0	0.5 to 1.5
4D5-8	1.0 to 2.0	0.5 to 1.5
4D5-9	0.5 to 1.0	>1.0
4D5-10	0.5 to 1.0	0.5 to 1.0
2C5-7	0.5 to 1.5	0.5 to 1.0
2C5-4	0.5 to 1.5	0.5 to 1.5

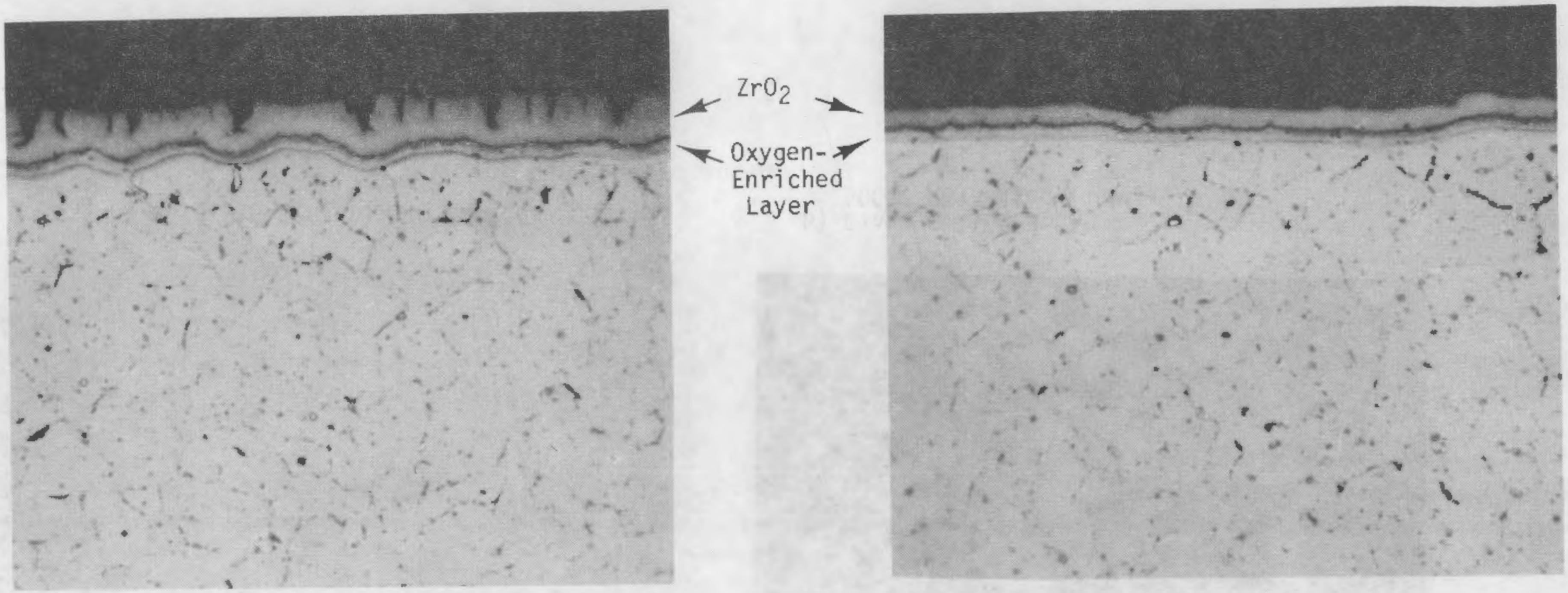

a) Plate C116-D3 - 1000X

b) Plate C116-D4 - 1000X

FIGURE 17. Typical Zirconium Oxide and Oxygen-Enriched Layers on the Outer (a) and Inner (b) Cladding Surfaces of All Rod Sections Examined Except 3C5-1, 3C5-9, 4C5-8 and 4C5-9

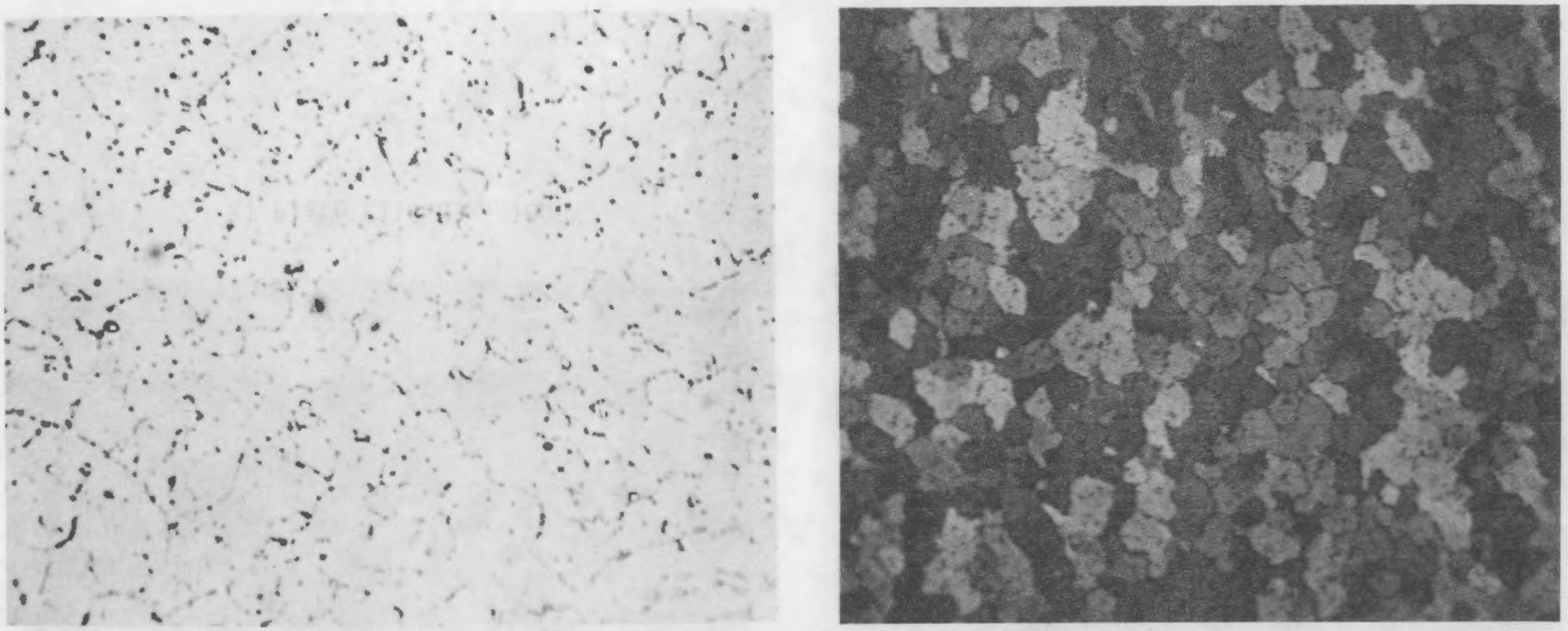

a) Plate C 116-E2 - 1000X

b) Plate C 116-E3
500X, Polarized Light

FIGURE 18. Typical Decorated Alpha Grain Boundaries of Rod Sections 4C5-4, 4D5-2, 4D5-3, 4D5-4, 4D5-5, and 4D5-6

During the early stage of oxidation, the parabolic rate constants of Zircaloy-2 and Zircaloy-4 are considered to be equal. With equal parabolic rate constants, the following relationship is derived to compare the zirconium oxide layer formation of Zircaloy-2 and Zircaloy-4.

$$\frac{\varepsilon_2}{\varepsilon_4} = \frac{t_2^{1/2}}{t_4^{1/2}} \quad (2)$$

where ε_2, ε_4, t_2, and t_4 are the thicknesses of and the time to form the zirconium oxide layers on the Zircaloy-2 and Zircaloy-4.

The length of time in which the fuel rods for the MT-3 test were at elevated temperatures (760 to 815°C) was estimated to be at least 150 s (Mohr et al. 1983). Other investigators have reported that the zirconium oxide layer formed on Zircaloy-2 after 10 min at 800°C was about 4.8 μm (Donaldson and Evans 1980). Using the above relationship, the calculated thickness of the zirconium oxide layer expected to form on the Zircaloy-4 cladding sections from the MT-3 test is about 2.4 μm. Thus, the calculated zirconium oxide thickness is less than what was actually observed, i.e., 2.4 μm versus an average of 3 to 6 μm. However, the calculated thickness does not account for zirconium oxide formed at times other than the 150 s at 760 to 810°C, such as pre-existing oxide and oxide formation during heating to test temperature and subsequent cooling to ambient temperatures. Thus the observed zirconium oxide thickness is consistent with the calculated thickness for Zircaloy-2 exposed to these conditions.

Figure 19 is a typical photomicrograph of the alpha grain growth observed in certain areas of Rod Sections 3C5-8, 3C5-9, 4C5-2, 4C5-3, 4C5-4, 4C5-6, 4D5-6, 4D5-7, 4D5-8, and 2C5-7 (Figures 4 through 8, 13, 14, and 16). Textural banding, which is the clustering of grains that are close to the same orientation, was observed in certain areas of Rod Sections 3C5-3, 3C5-4, 3C5-5, 4C5-5, 4C5-6, 4D5-5, 4D5-6, 4D5-7, 4D5-8, and 2C5-7 (Figures 2, 3, 8, 13, 14, and 16). Figure 20 is a representative photomicrograph of textural banding. Areas containing textural banding and alpha grain growth were observed in Rod Sections 4D5-6 and 4D5-8 (Figures 13, 14, and 21).

The cladding thickness was measured on each metallographic section at regular intervals around the circumference (cord of 0.040 in. or 1.02 mm) using the microscope viewing screen at 200X. These measurements are listed in Tables 4 through 19.

Particle size analyses were performed on the fragmented fuel from Sections 3C5, 4C5, and 4D5. The results are reported in Table 20 as percent of the total fuel weight retained by each sieve and the bottom receiver. The bulk of the fuel fragments (73.12%, 59.66%, and 56.68% from Rod Sections 3C5, 4C5, and 4D5, respectively) were retained on the 0.157-in. (4.0-mm) sieve. One pellet from Rod Section 3C5 remained intact following the sieve analysis, which indicates that the preconditioning phase of the test did not fragment all the UO_2 fuel pellets.

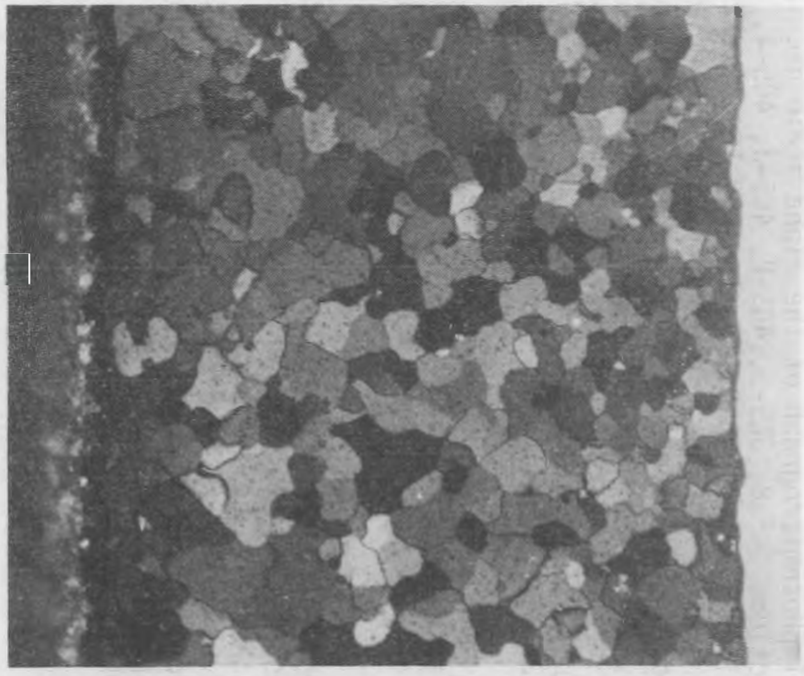

Plate C115-H4 - 200X

FIGURE 19. Typical Alpha Grain Growth of Rod Sections 3C5-8, 3C5-9, 4C5-2, 4C5-3, 4C5-4, 4C5-6, 4D5-6, 4D5-7, 4D5-8, and 2C5-7

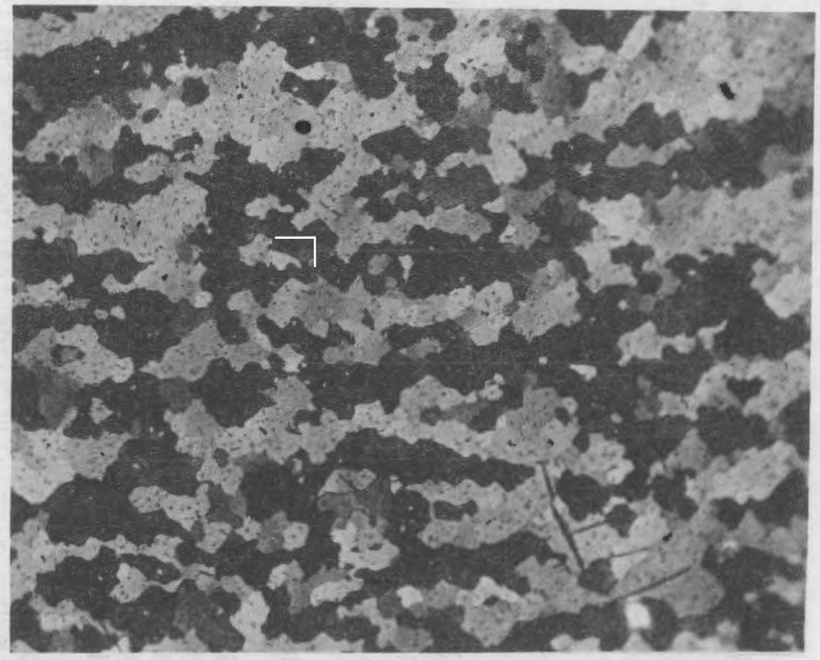

Plate C116-K4 - 500X

FIGURE 20. Typical Textural Banding of Rod Sections 3C5-3, 3C5-4, 3C5-5, 4C5-5, 4C5-6, 4D5-5, 4D5-6, 4D5-7, 4D5-8, and 2C5-7

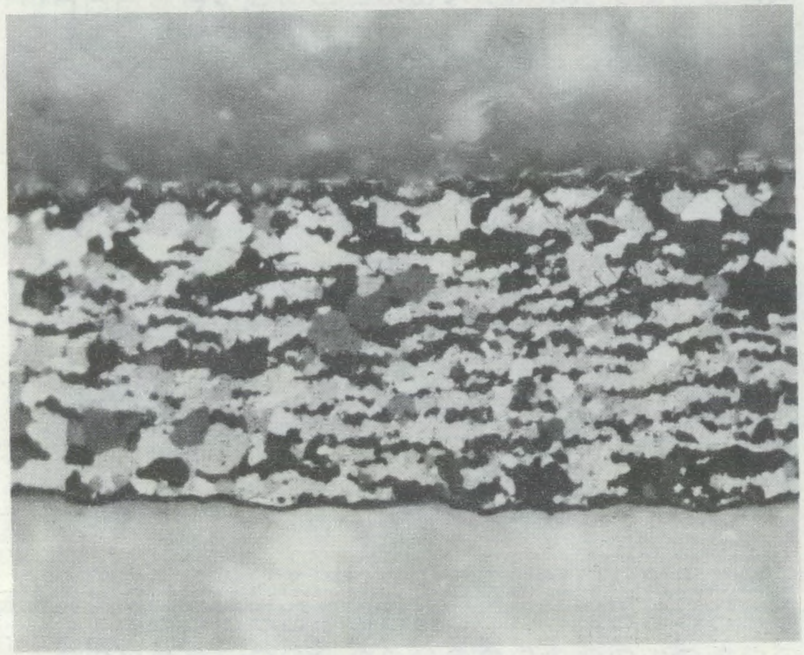

Plate C 116-K2 - 200X

FIGURE 21. Typical Areas Containing Alpha Grain Growth and Textural Banding of Rod Sections 4D5-6 and 4D5-8

TABLE 4. Cladding Thickness Measurements for Rod Sections 3C5-1 and 3C5-2[(a)]

3C5-1		3C5-2	
Distance from Reference Point,[(b)] in.	Wall Thickness, in.	Distance from Reference Point,[(b)] in.	Wall Thickness, in.
0.00	0.0220	0.00	0.0222
0.04	0.0224	0.04	0.0224
0.08	0.0224	0.08	0.0226
0.12	0.0223	0.12	0.0222
0.16	0.0224	0.16	0.0218
0.20	0.0225	0.20	0.0217
0.24	0.0223	0.24	0.0218
0.28	0.0220	0.28	0.0214
0.32	0.0220	0.32	0.0215
0.36	0.0220	0.36	0.0216
0.40	0.0216	0.40	0.0210
0.44	0.0214	0.44	0.0205
0.48	0.0216	0.48	0.0202
0.52	0.0215	0.52	0.0202
0.56	0.0213	0.56	0.0198
0.60	0.0213	0.60	0.0192
0.64	0.0212	0.64	0.0191
0.68	0.0207	0.68	0.0187
0.72	0.0203	0.72	0.0180
0.76	0.0205	0.76	0.0177
0.80	0.0208	0.80	0.0181
0.84	0.0209	0.84	0.0185
0.88	0.0212	0.88	0.0185
0.92	0.0216	0.92	0.0188
0.96	0.0214	0.96	0.0197
1.00	0.0213	1.00	0.0204
1.04	0.0219	1.04	0.0207
1.08	0.0222	1.08	0.0212
1.12	0.0224	1.12	0.0217
1.16	0.0226	1.16	0.0217
1.20	0.0228	1.20	0.0215
1.24	0.0225	1.24	0.0219
		1.28	0.0224

(a) See Figure 1 for reference points.
(b) Direction of travel - clockwise.

TABLE 5. Cladding Thickness Measurements for Rod Sections 3C5-3 and 3C5-4[a]

3C5-3		3C5-4	
Distance from Reference Point,[b] in.	Wall Thickness, in.	Distance from Reference Point,[b] in.	Wall Thickness, in.
0.00	0.0215	0.00	0.0205
0.04	0.0215	0.04	0.0202
0.08	0.0216	0.08	0.0199
0.12	0.0215	0.12	0.0200
0.16	0.0214	0.16	0.0191
0.20	0.0213	0.20	0.0180
0.24	0.0207	0.24	0.0175
0.28	0.0202	0.28	0.0174
0.32	0.0200	0.32	0.0170
0.36	0.0203	0.36	0.0164
0.40	0.0197	0.40	0.0167
0.44	0.0194	0.44	0.0172
0.48	0.0192	0.48	0.0174
0.52	0.0189	0.52	0.0168
0.56	0.0181	0.56	0.0165
0.60	0.0167	0.60	0.0165
0.64	0.0161	0.64	0.0169
0.68	0.0158	0.68	0.0167
0.72	0.0155	0.72	0.0165
0.76	0.0152	0.76	0.0165
0.80	0.0152	0.80	0.0166
0.84	0.0156	0.84	0.0168
0.88	0.0164	0.88	0.0164
0.92	0.0167	0.92	0.0158
0.96	0.0169	0.96	0.0160
1.00	0.0178	1.00	0.0169
1.04	0.0190	1.04	0.0175
1.08	0.0198	1.08	0.0179
1.12	0.0204	1.12	0.0188
1.16	0.0212	1.16	0.0197
1.20	0.0213	1.20	0.0200
1.24	0.0214	1.24	0.0203
1.28	0.0217	1.28	0.0205
		1.32	0.0205
		1.36	0.0210
		1.40	0.0209
		1.44	0.0207

(a) See Figure 2 for reference points.
(b) Direction of travel - clockwise.

TABLE 6. Cladding Thickness Measurements for Rod Sections 3C5-5 and 3C5-6[a]

3C5-5 Distance from Reference Point,[b] in.	3C5-5 Wall Thickness, in.	3C5-6 Distance from Reference Point,[b] in.	3C5-6 Wall Thickness, in.
0.00	0.0211	0.00	0.0219
0.04	0.0207	0.04	0.0213
0.08	0.0199	0.08	0.0212
0.12	0.0198	0.12	0.0211
0.16	0.0200	0.16	0.0210
0.20	0.0196	0.20	0.0206
0.24	0.0194	0.24	0.0204
0.28	0.0194	0.28	0.0204
0.32	0.0193	0.32	0.0198
0.36	0.0189	0.36	0.0195
0.40	0.0180	0.40	0.0196
0.44	0.0178	0.44	0.0199
0.48	0.0180	0.48	0.0195
0.52	0.0176	0.52	0.0191
0.56	0.0167	0.56	0.0191
0.60	0.0169	0.60	0.0190
0.64	0.0169	0.64	0.0185
0.68	0.0164	0.68	0.0182
0.72	0.0157	0.72	0.0188
0.76	0.0152	0.76	0.0197
0.80	0.0149	0.80	0.0200
0.84	0.0149	0.84	0.0207
0.88	0.0144	0.88	0.0214
0.92	0.0135	0.92	0.0216
0.96	0.0133	0.96	0.0214
1.00	0.0144	1.00	0.0216
1.04	0.0161	1.04	0.0221
1.08	0.0169	1.08	0.0220
1.12	0.0178	1.12	0.0222
1.16	0.0189	1.16	0.0224
1.20	0.0196	1.20	0.0225
1.24	0.0197	1.24	0.0221
1.28	0.0199		
1.32	0.0198		
1.36	0.0201		
1.40	0.0205		
1.44	0.0206		

(a) See Figure 3 for reference points.
(b) Direction of travel - clockwise.

TABLE 7. Cladding Thickness Measurements for Rod Sections 3C5-7 and 3C5-8[a]

3C5-7		3C5-8	
Distance from Reference Point,[b] in.	Wall Thickness, in.	Distance from Reference Point,[b] in.	Wall Thickness, in.
0.00	0.0202	0.00	0.0075
0.04	0.0197	0.04	0.0184
0.08	0.0195	0.08	0.0188
0.12	0.0194	0.12	0.0168
0.16	0.0191	0.16	0.0167
0.20	0.0192	0.20	0.0169
0.24	0.0191	0.24	0.0168
0.28	0.0188	0.28	0.0163
0.32	0.0179	0.32	0.0159
0.36	0.0176	0.36	0.0155
0.40	0.0181	0.40	0.0158
0.44	0.0184	0.44	0.0159
0.48	0.0180	0.48	0.0164
0.52	0.0177	0.52	0.0172
0.56	0.0177	0.56	0.0177
0.60	0.0179	0.60	0.0179
0.64	0.0178	0.64	0.0173
0.68	0.0177	0.68	0.0167
0.72	0.0177	0.72	0.0169
0.76	0.0186	0.76	0.0175
0.80	0.0191	0.80	0.0184
0.84	0.0190	0.84	0.0192
0.88	0.0196	0.88	0.0199
0.92	0.0204	0.92	0.0201
0.96	0.0209	0.96	0.0198
1.00	0.0211	1.00	0.0199
1.04	0.0212	1.04	0.0202
1.08	0.0218	1.08	0.0200
1.12	0.0217	1.12	0.0196
1.16	0.0214	1.16	0.0196
1.20	0.0217	1.20	0.0195
1.24	0.0218	1.24	0.0194
1.28	0.0216	1.28	0.0190
1.32	0.0216	1.32	0.0187
1.36	0.0214	1.36	0.0185
		1.40	0.0174
		1.44	0.0158
		1.48	0.0146
		1.52	0.0146
		1.56	0.0094
		1.60	0.0083

(a) See Figure 4 for reference points.
(b) Direction of travel - clockwise.

TABLE 8. Cladding Thickness Measurements for Rod Sections 3C5-9 and 3C5-10[(a)]

3C5-9		3C5-10	
Distance from Reference Point,[(b)] in.	Wall Thickness, in.	Distance from Reference Point,[(b)] in.	Wall Thickness, in.
0.00	0.0129	0.00	0.0215
0.04	0.0152	0.04	0.0219
0.08	0.0168	0.08	0.0219
0.12	0.0170	0.12	0.0221
0.16	0.0173	0.16	0.0224
0.20	0.0171	0.20	0.0225
0.24	0.0166	0.24	0.0224
0.28	0.0168	0.28	0.0224
0.32	0.0176	0.32	0.0227
0.36	0.0179	0.36	0.0227
0.40	0.0180	0.40	0.0228
0.44	0.0182	0.44	0.0229
0.48	0.0185	0.48	0.0229
0.52	0.0189	0.52	0.0227
0.56	0.0186	0.56	0.0226
0.60	0.0186	0.60	0.0227
0.64	0.0189	0.64	0.0227
0.68	0.0189	0.68	0.0227
0.72	0.0187	0.72	0.0228
0.76	0.0186	0.76	0.0229
0.80	0.0185	0.80	0.0227
0.84	0.0203	0.84	0.0227
0.88	0.0204	0.88	0.0226
0.92	0.0206	0.92	0.0223
0.96	0.0208	0.96	0.0220
1.00	0.0204	1.00	0.0219
1.04	0.0198	1.04	0.0220
1.08	0.0197	1.08	0.0219
1.12	0.0198	1.12	0.0219
1.16	0.0192	1.16	0.0219
1.20	0.0194	1.20	0.0218
1.24	0.0187	1.24	0.0216
1.28	0.0184		
1.32	0.0166		
1.36	0.0149		
1.40	0.0179		
1.44	0.0123		
1.48	0.0114		
1.52	0.0116		
1.56	0.0113		

(a) See Figure 5 for reference points.
(b) Direction of travel - clockwise.

TABLE 9. Cladding Thickness Measurements for Rod Sections 4C5-1 and 4C5-2[a]

4C5-1		4C5-2	
Distance from Reference Point,[b] in.	Wall Thickness, in.	Distance from Reference Point,[b] in.	Wall Thickness, in.
0.00	0.0206	0.00	0.0196
0.04	0.0210	0.04	0.0207
0.08	0.0214	0.08	0.0211
0.12	0.0222	0.12	0.0218
0.16	0.0229	0.16	0.0224
0.20	0.0230	0.20	0.0226
0.24	0.0234	0.24	0.0228
0.28	0.0234	0.28	0.0233
0.32	0.0234	0.32	0.0237
0.36	0.0233	0.36	0.0234
0.40	0.0237	0.40	0.0234
0.44	0.0240	0.44	0.0234
0.48	0.0237	0.48	0.0232
0.52	0.0235	0.52	0.0229
0.56	0.0233	0.56	0.0229
0.60	0.0229	0.60	0.0228
0.64	0.0229	0.64	0.0222
0.68	0.0222	0.68	0.0216
0.72	0.0219	0.72	0.0212
0.76	0.0213	0.76	0.0202
0.80	0.0210	0.80	0.0199
0.84	0.0207	0.84	0.0198
0.88	0.0202	0.88	0.0193
0.92	0.0192	0.92	0.0184
0.96	0.0190	0.96	0.0174
1.00	0.0185	1.00	0.0169
1.04	0.0182	1.04	0.0159
1.08	0.0181	1.08	0.0149
1.12	0.0188	1.12	0.0144
1.16	0.0194	1.16	0.0153
1.20	0.0197	1.20	0.0164
		1.24	0.0169
		1.28	0.0179

(a) See Figure 6 for reference points.
(b) Direction of travel - clockwise.

TABLE 10. Cladding Thickness Measurements for Rod Sections 4C5-3 and 4C5-4[a]

4C5-3		4C5-4	
Distance from Reference Point,[b] in.	Wall Thickness, in.	Distance from Reference Point,[b] in.	Wall Thickness, in.
0.00	0.0135	0.00	0.0037
0.04	0.0160	0.04	0.0069
0.08	0.0163	0.08	0.0098
0.12	0.0200	0.12	0.0123
0.16	0.0207	0.16	0.0144
0.20	0.0213	0.20	0.0169
0.24	0.0221	0.24	0.0185
0.28	0.0224	0.28	0.0195
0.32	0.0224	0.32	0.0207
0.36	0.0230	0.36	0.0217
0.40	0.0232	0.40	0.0222
0.44	0.0231	0.44	0.0221
0.48	0.0229	0.48	0.0222
0.52	0.0229	0.52	0.0222
0.56	0.0227	0.56	0.0219
0.60	0.0225	0.60	0.0222
0.64	0.0223	0.64	0.0225
0.68	0.0220	0.68	0.0224
0.72	0.0216	0.72	0.0221
0.76	0.0214	0.76	0.0218
0.80	0.0212	0.80	0.0214
0.84	0.0205	0.84	0.0209
0.88	0.0199	0.88	0.0209
0.92	0.0191	0.92	0.0208
0.96	0.0184	0.96	0.0203
1.00	0.0174	1.00	0.0199
1.04	0.0165	1.04	0.0194
1.08	0.0162	1.08	0.0189
1.12	0.0158	1.12	0.0180
1.16	0.0149	1.16	0.0173
1.20	0.0135	1.20	0.0169
1.24	0.0119	1.24	0.0162
1.28	0.0112	1.28	0.0148
1.32	0.0112	1.32	0.0134
1.36	0.0110	1.36	0.0124
1.40	0.0122	1.40	0.0115
		1.44	0.0108
		1.48	0.0099
		1.52	0.0072
		1.56	0.0047

(a) See Figure 7 for reference points.
(b) Direction of travel - clockwise.

TABLE 11. Cladding Thickness Measurements for Rod Sections 4C5-5 and 4C5-6[a]

4C5-5		4C5-6	
Distance from Reference Point,[b] in.	Wall Thickness, in.	Distance from Reference Point,[b] in.	Wall Thickness, in.
0.00	0.0114	0.00	0.0139
0.04	0.0123	0.04	0.0152
0.08	0.0137	0.08	0.0169
0.12	0.0159	0.12	0.0180
0.16	0.0169	0.16	0.0187
0.20	0.0179	0.20	0.0192
0.24	0.0183	0.24	0.0197
0.28	0.0204	0.28	0.0202
0.32	0.0212	0.32	0.0205
0.36	0.0213	0.36	0.0208
0.40	0.0217	0.40	0.0213
0.44	0.0222	0.44	0.0217
0.48	0.0219	0.48	0.0214
0.52	0.0219	0.52	0.0212
0.56	0.0219	0.56	0.0211
0.60	0.0219	0.60	0.0206
0.64	0.0218	0.64	0.0203
0.68	0.0218	0.68	0.0203
0.72	0.0219	0.72	0.0202
0.76	0.0217	0.76	0.0199
0.80	0.0212	0.80	0.0195
0.84	0.0209	0.84	0.0194
0.88	0.0205	0.88	0.0192
0.92	0.0201	0.92	0.0187
0.96	0.0201	0.96	0.0184
1.00	0.0200	1.00	0.0185
1.04	0.0197	1.04	0.0184
1.08	0.0190	1.08	0.0179
1.12	0.0184	1.12	0.0175
1.16	0.0174	1.16	0.0177
1.20	0.0164	1.20	0.0172
1.24	0.0156	1.24	0.0166
1.28	0.0153	1.28	0.0158
1.32	0.0152	1.32	0.0152
1.36	0.0144	1.36	0.0145
1.40	0.0126	1.40	0.0138
		1.44	0.0138

(a) See Figure 8 for reference points.
(b) Direction of travel - clockwise.

TABLE 12. Cladding Thickness Measurements for Rod Sections 4C5-7 and 4C5-8[a]

4C5-7		4C5-8	
Distance from Reference Point,[b] in.	Wall Thickness, in.	Distance from Reference Point,[b] in.	Wall Thickness, in.
0.00	0.0179	0.00	0.0207
0.04	0.0184	0.04	0.0208
0.08	0.0186	0.08	0.0207
0.12	0.0189	0.12	0.0202
0.16	0.0187	0.16	0.0201
0.20	0.0192	0.20	0.0205
0.24	0.0202	0.24	0.0208
0.28	0.0209	0.28	0.0209
0.32	0.0212	0.32	0.0209
0.36	0.0212	0.36	0.0210
0.40	0.0212	0.40	0.0212
0.44	0.0209	0.44	0.0209
0.48	0.0207	0.48	0.0206
0.52	0.0207	0.52	0.0205
0.56	0.0208	0.56	0.0204
0.60	0.0206	0.60	0.0201
0.64	0.0202	0.64	0.0202
0.68	0.0198	0.68	0.0202
0.72	0.0194	0.72	0.0201
0.76	0.0188	0.76	0.0197
0.80	0.0187	0.80	0.0194
0.84	0.0187	0.84	0.0194
0.88	0.0185	0.88	0.0192
0.92	0.0184	0.92	0.0196
0.96	0.0184	0.96	0.0199
1.00	0.0186	1.00	0.0202
1.04	0.0186	1.04	0.0201
1.08	0.0181	1.08	0.0201
1.12	0.0181	1.12	0.0200
1.16	0.0184	1.16	0.0199
1.20	0.0183	1.20	0.0198
1.24	0.0181	1.24	0.0204
1.28	0.0179	1.28	0.0209
1.32	0.0187	1.32	0.0207
1.36	0.0182		

(a) See Figure 9 for reference points.
(b) Direction of travel - clockwise.

TABLE 13. Cladding Thickness Measurements for Rod Section 4C5-9[a]

4C5-9	
Distance from Reference Point,[b] in.	Wall Thickness, in.
0.00	0.0238
0.04	0.0242
0.08	0.0239
0.12	0.0234
0.16	0.0233
0.20	0.0230
0.24	0.0227
0.28	0.0228
0.32	0.0229
0.36	0.0229
0.40	0.0224
0.44	0.0219
0.48	0.0219
0.52	0.0214
0.56	0.0214
0.60	0.0216
0.64	0.0217
0.68	0.0215
0.72	0.0216
0.76	0.0217
0.80	0.0219
0.84	0.0220
0.88	0.0224
0.92	0.0224
0.96	0.0225
1.00	0.0230
1.04	0.0231
1.08	0.0234
1.12	0.0235
1.16	0.0238
1.20	0.0234

(a) See Figure 10 for reference points.
(b) Direction of travel - clockwise.

TABLE 14. Cladding Thickness Measurements for Rod Sections 4D5-1 and 4D5-2[(a)]

405-1		405-2	
Distance from Reference Point,[(b)] in.	Wall Thickness, in.	Distance from Reference Point,[(b)] in.	Wall Thickness, in.
0.00	0.0219	0.00	0.0214
0.04	0.0219	0.04	0.0211
0.08	0.0217	0.08	0.0210
0.12	0.0215	0.12	0.0209
0.16	0.0215	0.16	0.0214
0.20	0.0217	0.20	0.0214
0.24	0.0218	0.24	0.0214
0.28	0.0217	0.28	0.0212
0.32	0.0215	0.32	0.0210
0.36	0.0214	0.36	0.0209
0.40	0.0215	0.40	0.0212
0.44	0.0217	0.44	0.0214
0.48	0.0219	0.48	0.0216
0.52	0.0218	0.52	0.0215
0.56	0.0218	0.56	0.0213
0.60	0.0219	0.60	0.0210
0.64	0.0220	0.64	0.0212
0.68	0.0224	0.68	0.0213
0.72	0.0225	0.72	0.0215
0.76	0.0224	0.76	0.0215
0.80	0.0223	0.80	0.0215
0.84	0.0224	0.84	0.0213
0.88	0.0225	0.88	0.0213
0.92	0.0227	0.92	0.0216
0.96	0.0228	0.96	0.0216
1.00	0.0227	1.00	0.0216
1.04	0.0224	1.04	0.0216
1.08	0.0222	1.08	0.0214
1.12	0.0220	1.12	0.0215
1.16	0.0220	1.16	0.0216

(a) See Figure 11 for reference points.
(b) Direction of travel - clockwise.

TABLE 15. Cladding Thickness Measurements for Rod Sections 4D5-3 and 4D5-4[a]

4D5-3		405-4	
Distance from Reference Point,[b] in.	Wall Thickness, in.	Distance from Reference Point,[b] in.	Wall Thickness, in.
0.00	0.0203	0.00	0.0183
0.04	0.0206	0.04	0.0187
0.08	0.0203	0.08	0.0188
0.12	0.0204	0.12	0.0194
0.16	0.0209	0.16	0.0199
0.20	0.0209	0.20	0.0205
0.24	0.0209	0.24	0.0204
0.28	0.0209	0.28	0.0204
0.32	0.0207	0.32	0.0204
0.36	0.0206	0.36	0.0204
0.40	0.0211	0.40	0.0207
0.44	0.0212	0.44	0.0211
0.48	0.0209	0.48	0.0213
0.52	0.0207	0.52	0.0210
0.56	0.0206	0.56	0.0209
0.60	0.0206	0.60	0.0208
0.64	0.0207	0.64	0.0209
0.68	0.0208	0.68	0.0212
0.72	0.0207	0.72	0.0209
0.76	0.0202	0.76	0.0206
0.80	0.0200	0.80	0.0205
0.84	0.0197	0.84	0.0200
0.88	0.0199	0.88	0.0194
0.92	0.0205	0.92	0.0196
0.96	0.0207	0.96	0.0199
1.00	0.0203	1.00	0.0197
1.04	0.0203	1.04	0.0192
1.08	0.0201	1.08	0.0193
1.12	0.0199	1.12	0.0191
1.16	0.0203	1.16	0.0189
1.20	0.0203	1.20	0.0191
1.24	0.0204	1.24	0.0194
		1.28	0.0191

(a) See Figure 12 for reference points.
(b) Oirection of travel - clockwise.

TABLE 16. Cladding Thickness Measurements for Rod Sections 4D5-5 and 4D5-6[a]

4D5-5		4D5-6	
Distance from Reference Point,[b] in.	Wall Thickness, in.	Distance from Reference Point,[b] in.	Wall Thickness, in.
0.00	0.0160	0.00	0.0126
0.04	0.0165	0.04	0.0141
0.08	0.0164	0.08	0.0155
0.12	0.0177	0.12	0.0174
0.16	0.0187	0.16	0.0186
0.20	0.0194	0.20	0.0189
0.24	0.0192	0.24	0.0187
0.28	0.0191	0.28	0.0184
0.32	0.0191	0.32	0.0184
0.36	0.0191	0.36	0.0182
0.40	0.0194	0.40	0.0191
0.44	0.0199	0.44	0.0195
0.48	0.0200	0.48	0.0201
0.52	0.0201	0.52	0.0202
0.56	0.0201	0.56	0.0206
0.60	0.0204	0.60	0.0108
0.64	0.0206	0.64	0.0212
0.68	0.0212	0.68	0.0216
0.72	0.0215	0.72	0.0219
0.76	0.0214	0.76	0.0218
0.80	0.0207	0.80	0.0217
0.84	0.0206	0.84	0.0217
0.88	0.0200	0.88	0.0210
0.92	0.0197	0.92	0.0209
0.96	0.0195	0.96	0.0207
1.00	0.0194	1.00	0.0199
1.04	0.0188	1.04	0.0186
1.08	0.0177	1.08	0.0177
1.12	0.0173	1.12	0.0160
1.16	0.0162	1.16	0.0142
1.20	0.0158	1.20	0.0138
1.24	0.0159	1.24	0.0136
1.28	0.0164	1.28	0.0134
1.32	0.0163	1.32	0.0134
1.36	0.0160	1.36	0.0128
1.40	0.0157	1.40	0.0116
		1.44	0.0112
		1.48	0.0118

(a) See Figure 13 for reference points.
(b) Direction of travel - clockwise.

TABLE 17. Cladding Thickness Measurements for Rod Sections 4D5-7 and 4D5-8[a]

4D5-7		4D5-8	
Distance from Reference Point,[b] in.	Wall Thickness, in.	Distance from Reference Point,[b] in.	Wall Thickness, in.
0.00	0.0094	0.00	0.0103
0.04	0.0109	0.04	0.0115
0.08	0.0129	0.08	0.0130
0.12	0.0153	0.12	0.0133
0.16	0.0169	0.16	0.0137
0.20	0.0177	0.20	0.0151
0.24	0.0178	0.24	0.0163
0.28	0.0176	0.28	0.0173
0.32	0.0174	0.32	0.0183
0.36	0.0176	0.36	0.0193
0.40	0.0182	0.40	0.0202
0.44	0.0184	0.44	0.0209
0.48	0.0189	0.48	0.0212
0.52	0.0194	0.52	0.0216
0.56	0.0203	0.56	0.0218
0.60	0.0206	0.60	0.0222
0.64	0.0214	0.64	0.0226
0.68	0.0221	0.68	0.0228
0.72	0.0223	0.72	0.0227
0.76	0.0223	0.76	0.0226
0.80	0.0221	0.80	0.0223
0.84	0.0218	0.84	0.0226
0.88	0.0218	0.88	0.0226
0.92	0.0217	0.92	0.0223
0.96	0.0217	0.96	0.0218
1.00	0.0208	1.00	0.0213
1.04	0.0201	1.04	0.0209
1.08	0.0185	1.08	0.0202
1.12	0.0170	1.12	0.0199
1.16	0.0158	1.16	0.0192
1.20	0.0150	1.20	0.0179
1.24	0.0142	1.24	0.0167
1.28	0.0128	1.28	0.0149
1.32	0.0112	1.32	0.0133
1.36	0.0097	1.36	0.0118
1.40	0.0094	1.40	0.0105
1.44	0.0096		
1.48	0.0091		

(a) See Figure 14 for reference points.
(b) Direction of travel - clockwise.

TABLE 18. Cladding Thickness Measurements for Rod Sections 4D5-9 and 4D5-10[a]

4D5-9		4D5-10	
Distance from Reference Point,[b] in.	Wall Thickness, in.	Distance from Reference Point,[b] in.	Wall Thickness, in.
0.00	0.0173	0.00	0.0209
0.04	0.0169	0.04	0.0209
0.08	0.0170	0.08	0.0207
0.12	0.0177	0.12	0.0208
0.16	0.0184	0.16	0.0212
0.20	0.0197	0.20	0.0215
0.24	0.0205	0.24	0.0219
0.28	0.0212	0.28	0.0220
0.32	0.0213	0.32	0.0222
0.36	0.0213	0.36	0.0224
0.40	0.0217	0.40	0.0226
0.44	0.0217	0.44	0.0231
0.48	0.0224	0.48	0.0233
0.52	0.0229	0.52	0.0231
0.56	0.0229	0.56	0.0231
0.60	0.0228	0.60	0.0231
0.64	0.0228	0.64	0.0232
0.68	0.0225	0.68	0.0235
0.72	0.0226	0.72	0.0235
0.76	0.0227	0.76	0.0233
0.80	0.0228	0.80	0.0230
0.84	0.0225	0.84	0.0228
0.88	0.0223	0.88	0.0228
0.92	0.0217	0.92	0.0226
0.96	0.0216	0.96	0.0224
1.00	0.0216	1.00	0.0220
1.04	0.0208	1.04	0.0216
1.08	0.0202	1.08	0.0212
1.12	0.0196	1.12	0.0210
1.16	0.0187	1.16	0.0212
1.20	0.0183		
1.24	0.0180		

(a) See Figure 15 for reference points.
(b) Direction of travel - clockwise.

TABLE 19. Cladding Thickness Measurements for Rod Section 2C5-7[a]

2C5-7	
Distance from Reference Point,[b] in.	Wall Thickness, in.
0.00	0.0034
0.04	0.0072
0.08	0.0098
0.12	0.0138
0.16	0.0165
0.20	0.0173
0.24	0.0183
0.28	0.0198
0.32	0.0211
0.36	0.0217
0.40	0.0220
0.44	0.0225
0.48	0.0225
0.52	0.0225
0.56	0.0229
0.60	0.0230
0.64	0.0229
0.68	0.0229
0.72	0.0225
0.76	0.0222
0.80	0.0219
0.84	0.0214
0.88	0.0209
0.92	0.0208
0.96	0.0204
1.00	0.0195
1.04	0.0194
1.08	0.0189
1.12	0.0181
1.16	0.0172
1.20	0.0171
1.24	0.0163
1.28	0.0140
1.32	0.0120
1.36	0.0112
1.40	0.0112
1.44	0.0094
1.48	0.0073
1.52	0.0048

(a) See Figure 16 for reference points.
(b) Direction of travel - clockwise.

TABLE 20. Fuel Particle Size Distribution of Fuel from Rod Sections 3C5, 4C5, and 4D5

Rod Section	Total Weight of Fuel, g	% of Total Sample Weight Retained on Each Sieve						
		No. 3-1/2 (0.233 in. or 5.6 mm)	No. 5 (0.157 in. or 4.0 mm)	No. 7 (0.111 in. or 2.8 mm)	No. 10 (0.0787 in. or 2.0 mm)	No. 18 (0.0394 in. or 1.0 mm)	No. 50 (0.0117 in. or 3.0 μm)	Receiver (<0.0117 in. or <3.0 μm)
3C5[a]	246.750	12.59	73.12	11.26	0.80	0.82	0.53	0.88
4C5	256.468	9.98	59.66	23.31	3.71	1.64	1.07	0.63
4D5	258.515	19.74	56.68	16.60	3.49	1.73	1.18	0.58

(a) One whole fuel pellet was present in the sample from Rod Section 3C5 before and after the sieve analysis.

REFERENCES

Chung, H. M., A. M. Garde, and T. F. Kassner. 1975. "Mechanical Properties of Zircaloy Containing Oxygen." In Light-Water-Reactor Safety Research Program: Quarterly Progress Report, April-June 1975. ANL-75-58, Argonne National Laboratory, Argonne, Illinois.

Donaldson, A. T., and H. E. Evans. 1980. Oxidation-Induced Creep in Zircaloy-2, Part 1: Basic Observations. RD/B/N4855, WR/FESG/P(80) 126, Berkeley Nuclear Laboratories, London, England.

Hann, C. R. 1979. Program Plan for LOCA Simulation in the National Research Universal (NRU) Reactor. PNL-3056, Pacific Northwest Laboratory, Richland, Washington.

Mohr, C. L., et al. 1983. LOCA Simulation in the National Research Universal Reactor Program - Data Report for the Third Materials Experiment (MT-3). NUREG/CR-2528, PNL-4166, Pacific Northwest Laboratory, Richland, Washington.

Picklesimer, M. L. 1957. Anodizing as a Metallographic Technique for Zirconium Base Alloys. ORNL-2296, Oak Ridge National Laboratory, Oak Ridge, Tennessee.

Rausch, W. N. 1984. LOCA Simulation in the National Research Universal (NRU) Reactor Program - Postirradiation Examination Results for the Third Materials Experiment (MT-3). NUREG/CR-3350, PNL-4933, Pacific Northwest Laboratory, Richland, Washington.

REFERENCES

Chung, H. M., A. M. Garde, and T. F. Kassner. 1978. "Mechanical Properties of Zircaloy Containing Oxygen." In Light-Water-Reactor Safety Research Program: Quarterly Progress Report, April-June 1975. ANL-75-58, Argonne National Laboratory, Argonne, Illinois.

Donaldson, A. T., and H. E. Evans. 1980. Oxidation-Induced Creep in Zircaloy-2, Part I: Basic Observations. RD/B/N-4725, TPRD/B/0/2/N80, Berkeley Nuclear Laboratories, London, England.

Hann, C. R. 1979. Program Plan for LOCA Simulation in the National Research Universal (NRU) Reactor. PNL-3056, Pacific Northwest Laboratory, Richland, Washington.

Mohr, C. L., et al. 1983. LOCA Simulation in the National Research Universal Reactor Program - Data Report for the Third Materials Experiment (MT-3). NUREG/CR-2528, PNL-4166, Pacific Northwest Laboratory, Richland, Washington.

Picklesimer, M. L. 1952. Anodizing as a Metallographic Technique for Zirconium Base Alloys. ORNL-2296, Oak Ridge National Laboratory, Oak Ridge, Tennessee.

Russcher, G. E. 1984. LOCA Simulation in the National Research Universal (NRU) Reactor Program - Postirradiation Examination Results for the Third Materials Experiment (MT-3). NUREG/CR-3594, PNL-4939, Pacific Northwest Laboratory, Richland, Washington.

DISTRIBUTION

No. of
Copies

OFFSITE

U.S. Nuclear Regulatory
Commission
Division of Technical
Information and Document
Control
7920 Norfolk Avenue
Bethesda, MD 20014

O. E. Bassett
U.S. Nuclear Regulatory
Commission
M/S P-1102
Washington, DC 20555

P. Boehnert
U.S. Nuclear Regulatory
Commission
Advisory Committee on Reactor
Safeguards
M/S H-1016
Washington, DC 20555

W. Hodges
U.S. Nuclear Regulatory
Commission
M/S P-1132
Washington, DC 20555

A. Hon
U.S. Nuclear Regulatory
Commission
M/S 1130-SS
Washington, DC 20555

No. of
Copies

W. Johnston
U.S. Nuclear Regulatory
Commission
M/S P-302
Washington, DC 20555

W. Kerr
U.S. Nuclear Regulatory
Commission
Advisory Committee on Reactor
Safeguards
M/S H-1016
Washington, DC 20555

N. Lauben
U.S. Nuclear Regulatory
Commission
M/S P-1132
Washington, DC 20555

G. Marino
U.S. Nuclear Regulatory
Commission
M/S 1130-SS
Washington, DC 20555

R. Meyer
U.S. Nuclear Regulatory
Commission
M/S 1130-SS
Washington, DC 20555

J. Norberg
U.S. Nuclear Regulatory
Commission
M/S NL 5650
Washington, DC 20555

No. of Copies		No. of Copies	
	L. Phillips U.S. Nuclear Regulatory Commission M/S P-924 Washington, DC 20555		N. Zuber U.S. Nuclear Regulatory Commission M/S 1130-SS Washington, DC 20555
	D. F. Ross U.S. Nuclear Regulatory Commission M/S 1130-SS Washington, DC 20555		B. Bingham Babcock and Wilcox Co. P.O. Box 1200 Lynchburg, VA 24505
	L. S. Rubenstein U.S. Nuclear Regulatory Commission M/S P-932 Washington, DC 20555		C. Morgan Babcock and Wilcox Co. P.O. Box 1200 Lynchburg, VA 24505
	P. Shewmon U.S. Nuclear Regulatory Commission Advisory Committee on Reactor Safeguards M/S H-1016 Washington, DC 20555	2	R. Duncan Combustion Engineering 1000 Prospect Hill Road P.O. Box 500 Windsor, CT 06095
	L. Shotkin U.S. Nuclear Regulatory Commission M/S 1130-SS Washington, DC 20555		S. Ritterbush Combustion Engineering 1000 Prospect Hill Road P.O. Box 500 Windsor, CT 06095
3	R. Van Houten U.S. Nuclear Regulatory Commission M/S 1130-SS Washington, DC 20555		L. P. Leach EG&G Idaho, Inc. P.O. Box 1625 Idaho Falls, ID 83401
	J. Voglewede U.S. Nuclear Regulatory Commission M/S P-924 Washington, DC 20555		P. E. McDonald EG&G Idaho, Inc. P.O. Box 1625 Idaho Falls, ID 83401
			D. Ogden EG&G Idaho, Inc. P.O. Box 1625 Idaho Falls, ID 83401
			P. Davis (ITI) Electric Power Research Institute 3412 Hillview Avenue Palo Alto, CA 94022

No. of Copies

R. Duffey
Electric Power Research Institute
3412 Hillview Avenue
Palo Alto, CA 94022

M. Merilo
Electric Power Research Institute
3412 Hillview Avenue
Palo Alto, CA 94022

R. Oehlberg
Electric Power Research Institute
3412 Hillview Avenue
Palo Alto, CA 94022

W. Sun
Electric Power Research Institute
3412 Hillview Avenue
Palo Alto, CA 94022

2 G. Thomas
Electric Power Research Institute
3412 Hillview Avenue
Palo Alto, CA 94022

L. Thompson
Electric Power Research Institute
3412 Hillview Avenue
Palo Alto, CA 94022

S. Armijo
General Electric Company
175 Curtner Avenue
San Jose, CA 95114

L. Noble
General Electric Company
175 Curtner Avenue
San Jose, CA 95114

No. of Copies

N. Shirley
General Electric Company
175 Curtner Avenue
San Jose, CA 95114

G. Sozzi
General Electric Company
175 Curtner Avenue
San Jose, CA 95114

R. Williams
General Electric Company
175 Curtner Avenue
San Jose, CA 95114

W. Kirchner
Los Alamos Scientific Laboratory
P.O. Box 1663
Los Alamos, NM 87544

D. M. Chapin
MPR Associates, Inc.
1140 Connecticut Avenue, NW
Washington, DC 20036

J. Davis
Nuclear Engineering Department
Potomac Electric Avenue, NW
Washington, DC 20068

2 R. Chapman
Oak Ridge National Laboratory
P.O. Box X
Oak Ridge, TN 37830

F. Mynatt
Oak Ridge National Laboratory
P.O. Box X
Oak Ridge, TN 37830

2 D. Burman
Westinghouse Electric Corporation
P.O. Box 355
Pittsburgh, PA 15230

No. of
Copies

2 L. D. Hochreiter
Westinghouse Electric
Corporation
P.O. Box 355
Pittsburgh, PA 15230

R. Rosal
Westinghouse Electric
Corporation
P.O. Box 355
Pittsburgh, PA 15230

FOREIGN

D. Hicks
AERE Harwell
Didcot, Oxon, OX11 ORA
England

M. D. Atfield
Chalk River Nuclear Laboratories
Atomic Energy of Canada, Ltd.
Chalk River, Ontario, Canada
KOJ 1JO

D. J. Axford
Chalk River Nuclear Laboratories
Atomic Energy of Canada, Ltd.
Chalk River, Ontario, Canada
KOJ 1JO

D. Hall
Chalk River Nuclear Laboratories
Atomic Energy of Canada, Ltd.
Chalk River, Ontario, Canada
KOJ 1JO

P. Fehrenbach
Chalk River Nuclear Laboratories
Atomic Energy of Canada, Ltd.
Chalk River, Ontario, Canada
KOJ 1JO

J. W. Logie
Chalk River Nuclear Laboratories
Atomic Energy of Canada, Ltd.
Chalk River, Ontario, Canada
KOJ 1JO

No. of
Copies

I. C. Martin
Chalk River Nuclear Laboratories
Atomic Energy of Canada, Ltd.
Chalk River, Ontario, Canada
KOJ 1JO

6 D. T. Nishimura
Chalk River Nuclear Laboratories
Atomic Energy of Canada, Ltd.
Chalk River, Ontario, Canada
KOJ 1JO

M.J.F. Notley
Chalk River Nuclear Laboratories
Atomic Energy of Canada, Ltd.
Chalk River, Ontario, Canada
KOJ 1JO

A. Okazaki
Chalk River Nuclear Laboratories
Atomic Energy of Canada, Ltd.
Chalk River, Ontario, Canada
KOJ 1JO

D. Thompson
Chalk River Nuclear Laboratories
Atomic Energy of Canada, Ltd.
Chalk River, Ontario, Canada
KOJ 1JO

A.T.D. Butland
203/A32
Atomic Energy Establishment,
Winfrith
Winfrith Heath
Dorchester
Dorset, England

R. Potter, 209/A32
Atomic Energy Establishment,
Winfrith
Winfrith Heath
Dorchester
Dorset, England

No. of
Copies

P. Coddington, 219/A32
Atomic Energy Establishment,
Winfrith
Winfrith Heath
Dorchester
Dorset, England

3 I. H. Gibson
Atomic Energy Establishment
Winfrith
Dorchester, Dorset DT2-8DH
England

4 T. Healey
Central Electricity Generating
Board
Berkeley Nuclear Laboratories
Berkeley, Gloucestershire GL13 9PB
England

F. Erbacher
Kernforschungzentrum Karlsruhe
Weberstrasse 5
75 Karlsruhe 1
Federal Republic of Germany

A. Fiege
Kernforschungzentrum Karlsruhe
Weberstrasse 5
75 Karlsruhe 1
Federal Republic of Germany

2 H. Rininslandd
Kernforschungzentrum Karlsruhe
Weberstrasse 5
75 Karlsruhe 1
Federal Republic of Germany

J. H. Gittus
SRD, Wigshaw Lane
Culcheth, Warrington, WA3 4VE
England

No. of
Copies

4 M. Ishikawa, Chief
Reactivity Accident Laboratory
Japan Atomic Energy Research
Institute
Tokai Research Establishment
Tokai-Mura, Naka-Gun
Ibaraki-Ken
Japan

S. Kawasaki
Fuel Reliability Lab III
Division of Reactor Safety
Japan Atomic Energy Research
Institute
Tokai Research Establishment
Tokai-Mura, Naka-Gun
Ibaraki-Ken
Japan

E. D. Hindle
UKAEA Springfields NPDL
Salwick, Preston, PR4 ORR
England

P. D. Parsons
UKAEA Springfields NPDL
Salwick, Preston, PR4 ORR
England

C. A. Mann
Springfields Nuclear Power
Development Laboratory
United Kingdom Atomic Energy
Authority
Springfields, Salwick
Preston PR 4 ORR
England

A. Garlick
United Kingdom Atomic Energy
Authority
The Reactor Group
Reactor Fuel Element Laboratories
Springfields, Salwick
Preston, England PR4 ORR

No. of Copies	
	ONSITE
4	Exxon Nuclear Company, Inc.
	T. Doyle
	W. Kayser
	J. Morgan
	W. Nechodom
50	Pacific Northwest Laboratory
	W. J. Bailey
	S. K. Edler
	M. D. Freshley

No. of Copies	
	R. L. Goodman
	J. H. Haberman (26)
	C. R. Hann
	G. M. Hesson
	U. P. Jenquin
	L. L. King
	R. R. Lewis
	L. J. Parchen
	F. E. Panisko (2)
	J. P. Pilger
	W. N. Rausch
	G. E. Russcher
	B. J. Webb
	N. J. Wildung
	Publishing Coordination (2)
	Technical Information (5)

NRC FORM 335 (2-84) NRCM 1102, 3201, 3202 U.S. NUCLEAR REGULATORY COMMISSION **BIBLIOGRAPHIC DATA SHEET** SEE INSTRUCTIONS ON THE REVERSE	1. REPORT NUMBER (Assigned by TIDC, add Vol. No., if any) NUREG/CR-4218 PNL-5433
2. TITLE AND SUBTITLE LOCA Simulation in the National Research Universal Reactor Program: Postirradiation Examination Results for the Third Materials Test (MT-3) - Second Campaign	3. LEAVE BLANK
	4. DATE REPORT COMPLETED MONTH: April YEAR: 1985
5. AUTHOR(S) J. H. Haberman	6. DATE REPORT ISSUED MONTH: June YEAR: 1985
7. PERFORMING ORGANIZATION NAME AND MAILING ADDRESS (Include Zip Code) Pacific Northwest Laboratory P.O. Box 999 Richland, WA 99352	8. PROJECT/TASK/WORK UNIT NUMBER
	9. FIN OR GRANT NUMBER B2277
10. SPONSORING ORGANIZATION NAME AND MAILING ADDRESS (Include Zip Code) Division of Accident Evaluation Office of Nuclear Regulatory Research U.S. Nuclear Regulatory Commission Washington, D.C. 20555	11a. TYPE OF REPORT Topical
	b. PERIOD COVERED (Inclusive dates)
12. SUPPLEMENTARY NOTES	

13. ABSTRACT (200 words or less)

A series of in-reactor experiments were conducted using full-length 32-rod pressurized water reactor (PWR) fuel bundles as part of the Loss-of-Coolant Accident (LOCA) Simulation Program by Pacific Northwest Laboratory (PNL). The third materials test (MT-3) was the sixth experiment in a series of thermal-hydraulic and materials deformation/rupture experiments conducted in the National Research Universal (NRU) Reactor, Chalk River, Ontario, Canada. The MT-3 experiment was jointly funded by the U.S. Nuclear Regulatory Commission (NRC) and the United Kingdom Atomic Energy Authority (UKAEA) with the main objective of evaluating ballooning and rupture during active two-phase cooling at elevated temperatures. All 12 test rods in the center of the 32-rod bundle failed with an average peak strain of 55.4%.

At the request of the UKAEA, a destructive postirradiation examination (PIE) was performed on 7 of the 12 test rods. The results of this examination were presented in a previous report. Subsequently, and at the request of UKAEA, PIE was performed on three additional rods along with further examination of one of the previously examined rods. Information obtained from the PIE included cladding thickness measurements, cladding metallography, and particle size analysis of the fractured fuel pellets. This report describes the additional PIE work performed and presents the results of the examinations.

14. DOCUMENT ANALYSIS – a. KEYWORDS/DESCRIPTORS		15. AVAILABILITY STATEMENT
Loss-of-Coolant Accident (LOCA)	alpha grain growth	Unlimited
Materials Test 3 (MT-3)	textural banding	
postirradiation examination (PIE)	prior beta phase	
cladding deformation/rupture		16. SECURITY CLASSIFICATION (This page) Unclassified (This report) Unclassified
b. IDENTIFIERS/OPEN-ENDED TERMS		17. NUMBER OF PAGES
		18. PRICE

*U.S. GOVERNMENT PRINTING OFFICE: 1985-461-721:20175